

# Noise Electrometry of Polar and Dielectric Materials

Rahul Sahay,<sup>1,2</sup> Satcher Hsieh,<sup>2,3</sup> Eric Parsonnet,<sup>2</sup> Lane W. Martin,<sup>3,4</sup>  
Ramamoorthy Ramesh,<sup>2,3,4</sup> Norman Y. Yao,<sup>2,3</sup> and Shubhayu Chatterjee<sup>2</sup>

<sup>1</sup>Department of Physics, Harvard University, Cambridge, Massachusetts 02138, USA

<sup>2</sup>Department of Physics, University of California, Berkeley, California 94720, USA

<sup>3</sup>Materials Sciences Division, Lawrence Berkeley National Laboratory, Berkeley, California 94720, USA

<sup>4</sup>Department of Materials Science and Engineering,  
University of California, Berkeley, California 94720, USA

A qubit sensor with an electric dipole moment acquires an additional contribution to its depolarization rate when it is placed in the vicinity of a polar or dielectric material as a consequence of electrical noise arising from polarization fluctuations in the material. Here, we characterize this relaxation rate as a function of experimentally tunable parameters such as sample-probe distance, probe-frequency, and temperature, and demonstrate that it offers a window into dielectric properties of insulating materials over a wide range of frequencies and length scales. We discuss the experimental feasibility of our proposal and illustrate its ability to probe a variety of phenomena, ranging from collective polar excitations to phase transitions and disorder-dominated physics in relaxor ferroelectrics. Our proposal paves the way for a novel table-top probe of polar and dielectric materials in a parameter regime complementary to existing tools and techniques.

Polar and dielectric materials exhibit a plethora of interesting correlated physics [1–4] and are emerging as key components in next-generation solid-state technologies [5–9]. As a consequence, a multitude of techniques for probing them have been developed, ranging from different forms of microscopy and spectroscopy to electrical transport (Fig. 1b) [10–16]. While these methods have led to incredible scientific progress, answering several prominent questions such as the origin of polar instabilities in ultra-thin ferroelectric films [9] and the structure of polar domains in relaxor ferroelectrics [17] remains a formidable challenge. In part, this is due to the difficulty of probing the near-equilibrium polar dynamics of thin samples over a wide range of length and time scales simultaneously [9] — which at present requires the use of high-intensity synchrotron light sources. As such, developing a table-top probe with the requisite frequency and spatial resolution would naturally complement existing experimental probes of polar and dielectric materials.

The advent of nanoscale quantum sensors, typically based upon impurities embedded in insulating materials, provides an avenue for developing such a probe. Such sensors are often excellent AC electrometers and magnetometers; they can probe a wide range of frequencies and can locally image both static configurations and dynamic fluctuations of electromagnetic fields with nanoscale resolution [18–23]. Indeed, a number of theoretical proposals and pioneering experiments have utilized their magnetic field sensing capabilities to probe spin dynamics and electrical current fluctuations in solid-state systems [21, 24–48].

In this Letter, we show that the *electrical* sensing capabilities of single-qubit sensors can be used to probe the near-equilibrium physics of polar and dielectric materials, even in the thin-film context. In particular, we demonstrate that the relaxation rate of a qubit in the presence of electrical noise arising from such materials encodes the material’s dielectric properties at frequencies set by the

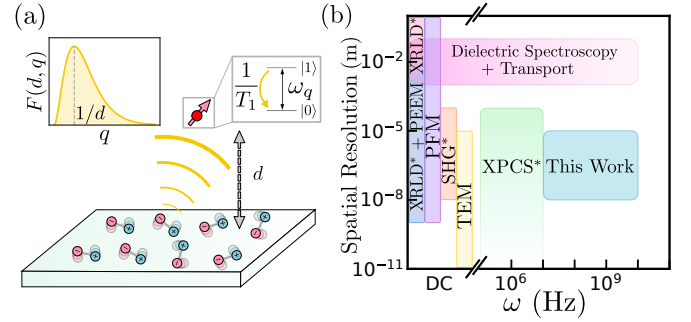


FIG. 1. (a) Schematic of qubit sensing experiment. A probe qubit (top right), with splitting  $\omega_q$ , is at a distance  $d$  away from a polar or dielectric material. Fluctuations in the material’s dipoles lead to electrical noise at the location of qubit causing the qubit to relax from  $|1\rangle$  to  $|0\rangle$  at a rate  $1/T_1$ . The qubit is sensitive to fluctuations at frequency  $\omega_q$  and wavevectors around  $1/d$  (see filter on top left). (b) Regimes of applicability of qubit sensors and other probes including microscopy techniques [atomic-force, piezoresponse-force, and transmission electron microscopy (AFM, PFM, and TEM)], spectroscopy techniques [x-ray photon correlation, x-ray linear dichroism, and second harmonic generation spectroscopy (XPCS, XRLD, and SHG)] and electrical transport techniques [10–16, 49]. Techniques that often require high intensity light sources are marked with a \*.

energy splitting of the qubit and wave vectors set by the qubit-sample distance. Hence, by tuning these two parameters, such qubit sensors can non-invasively and wirelessly probe polar and dielectric materials on frequency scales between 10 MHz – 10 GHz down to nanometer length scales and over a wide range of temperatures, 1 K – 600 K [50–52]. To highlight the utility of these sensors, we demonstrate how they can (i) detect the presence of exotic collective excitations in polar fluids, (ii) characterize paraelectric-to-ferroelectric phase transitions that underlie polar instabilities, and (iii) probe local polar dy-

namics in relaxor ferroelectrics. Finally, we illustrate the feasibility of qubit sensing via concrete numerical estimates for the relaxation rate of a nitrogen-vacancy (NV) center in diamond placed near a polar material (strontium titanate).

**Qubit Relaxometry Concept**—Our experimental proposal is depicted schematically in Fig. 1a wherein we envision an isolated impurity qubit sensor placed a distance  $d$  away from a polar or dielectric material. This qubit is a two-level system with a ground state  $|0\rangle$  split in energy from an excited state  $|1\rangle$  by  $\hbar\omega_q$  and its quantum state can be initialized, measured, and manipulated optically. Moreover, we consider qubits with an electric dipole moment  $\hat{\mathbf{d}} = d_\perp(\sigma_x\hat{x} + \sigma_y\hat{y})$  and a magnetic moment  $\hat{\boldsymbol{\mu}} = \mu_z\sigma_z\hat{z}$ , where  $\boldsymbol{\sigma}$  are the Pauli matrices, which specifies their coupling to electromagnetic fields as  $H_{\text{q-EM}} = \hat{\mathbf{d}} \cdot \mathbf{E} + \hat{\boldsymbol{\mu}} \cdot \mathbf{B}$ . As a result, electric fields  $\mathbf{E}$  drive transitions between  $|0\rangle$  and  $|1\rangle$  and magnetic fields  $\mathbf{B}$  can be utilized to control their frequency splitting. When placed close to a polar or dielectric material, electrical noise emanating from the material will couple the two states of the qubit and cause the qubit, initialized in its excited state, to naturally relax to a thermal equilibrium set by the ambient temperature,  $T$ . The rate of this relaxation can be expressed in terms of a time-scale  $T_1$  and can be computed from Fermi's Golden Rule as:

$$\frac{1}{T_1} = \frac{d_\perp^2}{2} \coth\left(\frac{\beta\omega_q}{2}\right) \int_{-\infty}^{\infty} dt \langle [E_-(t), E_+(0)] \rangle e^{i\omega_q t} \quad (1)$$

where the electrical noise is quantified via the auto-correlation function  $\langle [E_-(t), E_+(0)] \rangle$  with  $E_\pm = E_x \pm iE_y$ ,  $\beta = 1/k_B T$ , and  $\langle \cdots \rangle$  denotes thermal averaging. Intuitively, Eq. (1) expresses that only electrical noise at a frequency resonant with the splitting of the qubit contributes to its relaxation rate.

To understand how the relaxation rate is connected to the dielectric properties of the underlying material, we note that the electrical noise responsible arises from thermal or quantum fluctuations of the material's polarization density  $\mathbf{P}$ . The fluctuations at frequency  $\omega$  and wavevector  $\mathbf{q}$  can be quantified by the retarded polarization correlation function  $\chi_{\alpha\beta}(\omega, \mathbf{q}) = i \int_0^\infty dt e^{i\omega t} \langle [P_\alpha^\dagger(t, \mathbf{q}), P_\beta(0, \mathbf{q})] \rangle$  ( $\alpha, \beta = x, y, z$ ) which determines the dielectric tensor of the material,  $\varepsilon_{\alpha\beta}(\omega, \mathbf{q})$ , and thus encodes its electrical response [53–55]. By utilizing these correlation functions, we can formalize the relationship between fluctuations of polarization in the material and electrical noise at the qubit. For simplicity, we assume that the material is a stack of  $N$ , weakly inter-correlated, two-dimensional (2D) monolayers spaced apart by a distance  $w$  (modeling a thin-film) and is both translationally and rotationally invariant (see supplementary material for generalizations) [56]. From Maxwell's equations, polarization fluctuations of this sample propagate to electrical noise as:

$$\langle [E_-(t), E_+(0)] \rangle = \mu_0^2 \int \frac{d\omega d^2\mathbf{q}}{(2\pi)^3} F(d, q) \mathcal{C}(\omega, \mathbf{q}) e^{-i\omega t} \quad (2)$$

where  $\mathcal{C}(\omega, \mathbf{q}) = \text{Im} [\chi_{+-}(\omega, \mathbf{q}) + \chi_{-+}(\omega, \mathbf{q}) + 4\chi_{zz}(\omega, \mathbf{q})]$ , and  $F(d, q) = \sum_{j=0}^{N-1} q^2 e^{-2q(d+jw)}/16$  filters polarization fluctuations at different wavevectors. Crucially,  $F(d, q)$  is sharply peaked at  $1/d$  and so the qubit will only see fluctuations in the polarization around this wavevector. By combining Eqs. (1) and (2), we find that:

$$\frac{1}{T_1} = \frac{d_\perp^2 \mu_0^2}{2} \coth\left(\frac{\beta\omega_q}{2}\right) \int \frac{d^2\mathbf{q}}{(2\pi)^2} F(d, q) \mathcal{C}(\omega_q, \mathbf{q}) \quad (3)$$

Therefore, by tuning the frequency splitting of the qubit  $\omega_q$  and the qubit-sample distance  $d$ , one can effectively reconstruct the functional form of  $\mathcal{C}(\omega, \mathbf{q})$  [57]. Thus, measuring the qubit's relaxation rate gives one access to the dielectric properties of a proximate material.

A few remarks are in order. First, we note that existing qubit sensing setups have demonstrated the capability to tune a probe qubit's frequency between 10 MHz–10 GHz, have reached qubit-sample distances down to  $\sim 10$  nm, and have operated between 1 – 600 K [58–60]. The parameter regimes accessible by qubit sensors and other equilibrium/near-equilibrium probes of polar and dielectric materials are depicted in Fig. 1b [10–16, 49, 56] which highlights that our probe can nicely complement existing experimental techniques. Second, we note that the frequency scales accessible to qubit sensors are small relative to the excitation energy scales of typical materials. As a result, they will be sensitive to gapless or weakly gapped polar excitations.

**Applications**—The ability to probe such excitations naturally enables qubit sensors to address questions about polar and dielectric materials relevant to both fundamental and applied science. We examine in detail three such questions.

To begin, we discuss how the qubit sensor can detect collective modes in neutral polar fluids. While the existence of “plasmon” collective modes, arising from long-range Coulomb interactions between charged electrons in metals, has been well established [61], the conclusive observation of their dipolar analogues—“dipolarons”—has remained an outstanding challenge [62–64]. Dipolarons in a 2D dipolar fluid with density  $n_d$ , molecular mass  $m$ , and dipole moment  $\boldsymbol{\mu}$  are predicted to be gapless [56, 62] with an unusual dispersion  $\omega_d^2(\mathbf{q}) = v^2 q^2 + 2\pi n_d q(\mathbf{q} \cdot \boldsymbol{\mu})^2/m$ , which is anisotropic due to the directional dependence of the dipolar interaction. Dispersion in hand, we can predict the frequency and distance scaling of the relaxation rate  $1/T_1$  of a nearby qubit. In particular, for a general polar mode with dispersion  $\omega(\mathbf{q})$  and gap  $\omega_0$ , the polarization correlations take the form  $\chi_{-+}(\omega, \mathbf{q}) \sim (\omega - \omega(\mathbf{q}) + i0^+)^{-1}$  and hence  $1/T_1$  is given by [56, 65]:

$$\frac{1}{T_1} \sim \coth\left(\frac{\beta\omega_q}{2}\right) \times [e^{-2q_{\text{res}}d} q_{\text{res}}^2] \Theta(\omega_q - \omega_0) \quad (4)$$

where  $q_{\text{res}}$  satisfies  $\omega(q_{\text{res}}) = \omega_q$ . Thus, for gapless dipolarons in particular, the crossover from a linear to  $q^{3/2}$  dispersion with increasing  $q$  manifests in a corresponding crossover in the frequency scaling of  $1/T_1$  from

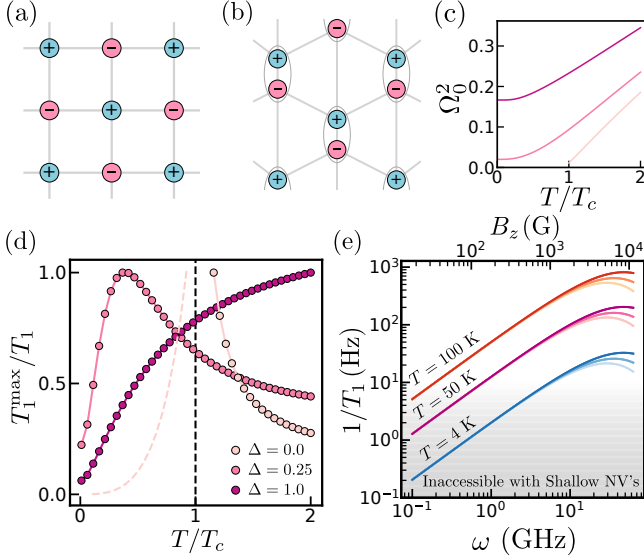


FIG. 2. (a, b) Schematic of ionic crystal in the (a) PE phase and the (b) FE phase. (c, d) Behavior of  $1/T_1$  across a relaxor ferroelectric for disorder  $\Delta = 0.0, 0.25, 1.0$  (see Panel (d) for legend). The presence of disorder causes a polarization-carrying mode to open a gap which can drastically change the response of qubit sensors. (e) Numerical estimate for  $1/T_1^{\text{sig}}$  compared to intrinsic relaxation rate of the NV qubit as a function of frequency,  $\omega$ , and applied magnetic field,  $B_z$ .  $1/T_1$  is depicted for temperatures  $T = 4$  K, 50 K, 100 K (shown in blue, purple, and red respectively) and distances  $d = 30, 50, 70$  nm (depicted as shading from dark to light). For all parameters shown, the relaxation rate is above experimental limits of  $1/T_1$  determined in Ref. [68].

$\omega_q e^{-2\omega_q d/v}$  to  $\sim \omega_q^{1/3} e^{-2(\omega_q)^{2/3} d}$ , and can serve as a smoking gun signature of these collective modes.

The ability to probe low-energy polar excitations further enables qubit sensors to characterize phase transitions in polar and dielectric materials. While such transitions are well-understood in three dimensions (3D), their nature is unclear in 2D; coupling to additional low-energy modes, irrelevant in 3D, could dramatically alter the universal properties of the transition [66]. Furthermore, previous experiments aimed at fabricating thin-film ferroelectrics for device applications have encountered instabilities in the material’s polarization, suspected to be intimately related to the stability of the 2D paraelectric to ferroelectric (PE/FE) phase transition [67]. Motivated by these outstanding questions, we make predictions for the behavior of  $1/T_1$  across a continuous PE/FE phase transition.

The PE/FE transition is a structural phase transition accompanied by inversion-symmetry breaking and a spontaneously generated polarization density. It can be visualized by considering an ionic crystal with alternating charges  $\pm Q$  shown in both the PE and FE phase in Fig. 2(a, b) respectively. This transition is driven by the softening of transverse optical phonon modes which correspond to the relative displacement between the  $\pm Q$

charges depicted. The mechanism underlying this softening is either thermal or quantum fluctuations depending on whether the transition is driven by temperature (a “thermal phase transition”) or a separate tuning parameter  $\lambda$  (e.g. strain) at  $T = 0$  (a “quantum phase transition”) [61, 69]. If we assume that these phonon modes do not interact and have dispersion  $\omega^2(\mathbf{q}) = c_s^2 \mathbf{q}^2 + \omega_0^2$  with  $\omega_0 \rightarrow 0$  at the transition, from Eq. (4) we find that once  $\omega_0$  is less than the frequency splitting of the qubit, the qubit sensor will detect its presence. Although interactions will dramatically affect the polarization correlations near the transition and hence the scaling of  $1/T_1$ , this simple analysis illustrates that qubit sensors are ideal for probing the critical physics around the transition. This motivates a more careful analysis of  $1/T_1$  around a critical point by using dynamical scaling theories for both thermal and quantum transitions [61].

Around the critical point  $\lambda = \lambda_c$ , the static correlations of the polarization are set by a diverging correlation length  $\xi \propto |\lambda - \lambda_c|^{-\nu}$ , while dynamics are strongly constrained by symmetries. Since the polarization density is not conserved, the corresponding dynamics are relaxational, characterized by an order-parameter relaxation rate  $\Gamma$ . A key difference between thermal and quantum phase transitions is how they behave upon changing  $T$  in the vicinity of the critical point. Thermal transitions are driven by  $T$  and hence both  $\xi$  and  $\Gamma$  scale as a power law of the distance from the critical point  $t = (T - T_c)/T_c$ . Consequently, we can conclude using the dynamic scaling theory of critical phenomena [56, 70–73] that:

$$\frac{1}{T_1} \sim \frac{2T}{d^{2+\eta-z}} \Psi_t \left( \omega d^z, \frac{\xi}{d} \right), \quad \xi \propto |t|^{-\nu} \quad (5)$$

where  $\Psi_t$  is a scaling function,  $\eta$ ,  $\nu$ , and  $z$  are critical exponents. If  $\Psi_t$  is smooth in the  $\omega \rightarrow 0$  limit, then  $1/T_1$  scales with qubit-sample distance as  $d^{-2-\eta+z}$  at the critical point in stark contrast to the non-critical regime where it scales as  $1/d^4$ ; a change in the distance dependence of  $T_1$  is a tell-tale signature of approaching thermal criticality. In addition, a scaling analysis near  $T_c$  enables extracting critical exponents  $\eta$ ,  $z$  and  $\nu$ . On the other hand, if we tune to a quantum critical point ( $\lambda = \lambda_c$ ) and raise  $T$  from 0 K, then the lack of any gap scale in the spectrum ( $\omega_0 = 0$ ) implies that both the correlation length  $\xi \sim c_s/T^{1/z}$  and relaxation rate  $\Gamma \sim T$  are solely determined by temperature. This can be used to show that  $1/T_1$  scales as a power law in  $T$  (rather than  $T - T_c$ ), with a distinct distance dependence [56, 61, 74]:

$$\frac{1}{T_1} \propto \begin{cases} T^{(2+\eta)/z} \log \left( \frac{c_s}{dT^{1/z}} \right), & d \ll \xi \\ T^{(-2+\eta)/z} d^{-4}, & d \gg \xi. \end{cases} \quad (6)$$

While the distance-scaling of  $1/T_1$  informs us of whether we are in the critical regime, its temperature-scaling can be used to determine the critical exponents  $\eta$  and  $z$ . Finally, the dependence of the spectral gap  $\omega_0 \propto |\lambda - \lambda_c|^{\nu z}$  on the tuning parameter  $\lambda$ , derived from low-T activated

behavior of  $1/T_1$ , may be used to deduce the critical exponent,  $\nu$ . Thus, all critical exponents for the quantum transition may be deduced by an analysis of the qubit's relaxation rate as a function of  $T$ ,  $d$  and  $\lambda - \lambda_c$ .

Up until this point, we have explored clean systems without quenched disorder. However, it is known that disorder can dramatically affect the behavior of low-dimensional materials [75]. A prototypical example is in relaxor ferroelectrics (relaxors), dielectric materials characterized by anomalously large internal polar fluctuations resembling “disorder broadened” critical correlations of phase transitions [76–80]. While a full microscopic description of relaxors is missing, their properties are often attributed to competition between the long-range dipolar interaction, which orders internal dipoles, and short-range disorder, which freezes them in a particular direction [80–82]. This competition is captured by a minimal classical model of dipoles arranged in a 2D lattice [82, 83]:

$$H = \sum_i \left[ \frac{\Pi_i^2}{2M} + V(u_i) - h_i u_i \right] - \sum_{i < j} v_{ij} u_i u_j \quad (7)$$

where  $\Pi_i = M\dot{u}_i$  is the conjugate momentum of the polarization-carrying displacement  $u_i$  chosen to be along the  $z$ -axis,  $M$  is the effective mass,  $v_{ij}$  is the dipolar interaction,  $h_i$  is a normally distributed random field with width  $\Delta$ , and  $V(u_i) = \frac{\kappa}{2}u_i^2 + \frac{\gamma}{4}u_i^4$  ( $\kappa, \gamma > 0$ ) is an anharmonic potential. When our impurity qubit is far from the material ( $d \gg \sqrt{A}$  where  $A$  is the area of a polar region), the qubit is insensitive to the local realization of  $h_i$  and encodes the disorder-averaged dynamics of the relaxor. Here, the polarization correlations take a damped harmonic form  $\chi_{zz}(\omega, \mathbf{q}) = (M\Omega^2(\mathbf{q}) - M\omega^2 + i\omega\Gamma)^{-1}$  where  $\Omega^2(\mathbf{q}) = \Omega_0^2 + (v_0 - v_{\mathbf{q}})$ ,  $v_{\mathbf{q}}$  is the Fourier transformed dipolar interaction,  $v_0 = \lim_{\mathbf{q} \rightarrow 0} v_{\mathbf{q}}$ ,  $\Gamma$  is a phenomenological damping, and  $\Omega_0$  is determined self-consistently in a mean-field analysis and is depicted in Fig. 2(c) in the clean, weak disorder, and strong disorder case ( $\Delta = 0, 0.25, 1.0$ , respectively) [56, 80–82, 84, 85]. From the mode frequency  $\Omega_0^2$  at  $\Delta = 0$ , we can extract a critical temperature  $T_c$  defined as the temperature where the mode becomes massless. Mode frequency and critical temperature in hand, we numerically compute  $1/T_1$  in a temperature range around  $T = T_c$  and normalize  $1/T_1$  by its maximum in that range,  $1/T_1^{\max}$  (Fig. 2(d)). We find that, in the clean case  $\Delta = 0$ , the relaxation rate becomes sharply peaked at the location of the phase transition, whereas for weak disorder ( $\Delta = 0.25$ ) the response broadens, reproducing our earlier intuition. For sufficiently large disorder, the peak is removed entirely and the relaxation rate increases monotonically on lowering  $T$ .

On the other hand, when our impurity qubit is sufficiently close to the material ( $d \sim \sqrt{A}$ ), the qubit will be able to resolve the microscopic dynamics of individual polar domains and the assumption of translation invariance of Eq. 3 will no longer hold. Here we present a qualitative picture of the physics made accessible by spatio-

temporally resolving these polar dynamics. Relaxor ferroelectrics are often modeled using polar nano-regions — static nanoscale polar domains with non-zero spontaneous polarization pinned by disorder [86–88]. The presence of such polar nano-regions with quenched fluctuations would imply a suppressed  $1/T_1$  once the qubit is positioned on top of such a region, and enhanced  $1/T_1$  when the qubit lies close to a domain wall. On the other hand, recent works have suggested a ‘slush-water’ picture of relaxors [17] characterized by coexisting static (ice-like) domains with frozen moments and dynamic (water-like) domains with fluctuating polarization; above an ice-like domain,  $1/T_1$  would be suppressed, while above a water-like domain,  $1/T_1$  would be enhanced. By studying  $1/T_1$  of an isolated qubit as a function of in-plane coordinates at a fixed distance  $d \lesssim \sqrt{A}$ , a spatially resolved map of the static and dynamic domains in an inhomogeneous sample could be obtained and aid in evincing a microscopic description of relaxors.

*Experimental Realization and Feasibility*—While our previous discussion has theoretically motivated the utility of qubit sensing in probing polar and dielectric materials, here we discuss a concrete realization of the qubit sensing setup and its feasibility. In particular, we envision utilizing the NV center in diamond: a point defect consisting of a nitrogen substitution adjacent to a lattice vacancy defect. The  $^3A_2$  electronic spin manifold of the NV is modeled as a three-level system ( $|0\rangle$ ,  $|+\rangle$ , and  $|-\rangle$ ) and the degenerate  $|\pm\rangle$  states are ideal for encoding the two-level qubit of our proposal [89]. Crucially, these degenerate states can be initialized and manipulated optically and read-out through state-dependent fluorescence [90]. Moreover, as required, electric fields drive transitions between these states with dipole moment  $d_{\perp} = 17 \text{ Hz} \cdot \text{cm/V}$  and magnetic fields control their splitting with a magnetic moment of  $\mu_z = 2.8 \text{ MHz/G}$  [90, 91]. As a result, the splitting of the NV can be controlled by local magnetic fields and the qubit-sample distance can be controlled by, for example, placing a nano-diamond with a single NV on a scanning probe tip [24, 28, 32, 35], enabling a measurement of  $1/T_1$  as a function of both frequency and distance.

To assess the feasibility of this proposal, we express the relaxation rate of the NV as  $T_1^{-1} = (T_1^{\text{sig}})^{-1} + (T_1^{\text{int}})^{-1}$ , where  $(T_1^{\text{sig}})^{-1}$  accounts for the signal from the sample and  $(T_1^{\text{int}})^{-1}$  accounts for intrinsic sources of relaxation from the diamond host, whose magnitude establishes a limit on the sensitivity of our sensing protocol. The magnitude of  $(T_1^{\text{int}})^{-1}$  has been reported in shallow NV samples ( $\sim 50 \text{ nm}$  depth) as low as  $10 \text{ Hz}$  below  $100 \text{ K}$  [68, 92]. The feasibility of our proposal can be established by comparing this noise floor to the expected signal magnitude in a paradigmatic setting: the ionic crystal model introduced earlier with a density  $\rho$ , lattice spacing  $a$  (See Fig. 2(a,b)), and polarization-carrying phonon mode with dispersion  $\omega_d(\mathbf{q}) = \sqrt{c_s^2 q^2 + \omega_0^2}$  with  $c_s$  equal to the mode speed. In this case,  $(T_1^{\text{sig}})^{-1}$  takes the form of Eq. 4 with a di-



mensionful multiplier  $\mathcal{N} = (\pi/2c_s^2) \times (\mu_0^2 d_\perp^2 c^4/64\pi) \times [(Q^2/a^4) \times (\hbar/\rho)]$  [56]. Choosing material parameters  $\{a, \rho, c_s, \omega_0, Q, w, N\} = \{0.3905 \text{ nm}, 183 \text{ amu}/a^2, 7.5 \cdot 10^3 \text{ m/s}, 0 \text{ GHz}, 9.66 \text{ e}, a, 300 \text{ layers}\}$ , motivated from a representative dielectric material (thin-film strontium titanate) [93–95], we can now compare  $(T_1^{\text{sig}})^{-1}$  as a function of frequency, distance, and temperature, to our noise floor,  $(T_1^{\text{int}})^{-1}$  as depicted in Fig. 2(e). For the parameters chosen, the signal magnitude is found to be significantly larger than currently accessible NV intrinsic relaxation rates over a wide range of temperatures and frequencies.

We note that in our feasibility analysis, we assumed that excitations above the ground state are non-interacting and long-lived. While this assumption only holds in the limit of dilute excitations, we expect that the presence of interactions will enhance polarization fluctuations. Hence, our estimate is expected to be a lower bound on the relaxation rate and motivates the feasibility of our method generally. We also remark that we have neglected the contribution of magnetic noise, which induces decay from the NV’s  $|\pm 1\rangle$  states to  $|0\rangle$ . While this is appropriate when probing insulating materials because the relaxation rate due to magnetic noise generated from electrical dipoles is smaller than the electrical noise by a factor of  $\mu_z^2 c_s^2/d_\perp^2 c^4 \sim 10^{-4} \ll 1$  [56], it is not in general true for metals, where the relaxation rate will be dominated by current fluctuations of itinerant electrons.

*Conclusions*— In this work, we demonstrated that qubit sensors are a promising table-top tool for studying near-equilibrium dynamics in polar and dielectric materials and can probe even thin-film samples over a wide range of frequencies ( $\sim 10 \text{ MHz} - 10 \text{ GHz}$ ) and temperatures ( $1 - 600 \text{ K}$ ) down to the nanometer scale. These capabilities make such sensors sensitive to low energy polar modes, enabling them to probe a variety of physical phenomena, ranging from collective polarization modes in long-range interacting systems, to paraelectric-to-ferroelectric phase transitions and disorder-induced phenomena in relaxor ferroelectrics. Complementary to existing techniques, the nanoscale spatial resolution of qubit sensors allows us to probe local dynamics in inhomogeneous materials. We briefly comment on a few open directions involving qubit electrometry. First, since

previous work has demonstrated the sensing capabilities of impurity qubits at high pressures ( $\sim \mathcal{O}(10) \text{ GPa}$ ), such qubits could naturally investigate the influence of pressure and strain fields on the dynamics of polarization and could aid in characterizing strain-induced phase transitions [96–98]. In addition, as illustrated in Eq. (3), our qubit probe is more sensitive to surface physics at short sample-probe distances [56]. Consequently, it can be used to resolve surface polarization dynamics, which can be distinct from the bulk [99]. The nanoscale resolution of the qubit is ideally suited to probe unconventional ferroelectricity in moiré materials, which typically have superlattice lengthscales of tens of nanometers [100, 101]. Finally, by using the electrical capabilities of qubit sensors, highlighted in this work, with the previously established magnetic capabilities, one may be able to probe the complex interplay between charge, polarization, and magnetization found in multiferroic materials [1].

*Acknowledgments*— We gratefully acknowledge discussions with Eugene Demler, Marcin Kalinowski, Francisco Machado, Thomas Mittiga, Joaquin Rodriguez-Nieva, Eric Peterson, Lokeshwar Prasad, and Chong Zu. We would especially like to thank Eugene Demler, Francisco Machado, and Joaquin Rodriguez-Nieva for collaborations on related projects. R.S. acknowledges support from the Barry M. Goldwater Scholarship, UC Berkeley’s Summer Undergraduate Research Fellowship, and by the U.S. Department of Energy, Office of Science, Office of Advanced Scientific Computing Research, Department of Energy Computational Science Graduate Fellowship under Award Number DESC0022158. S.C. was supported by the ARO through the Anyon Bridge MURI program (grant number W911NF-17-1-0323) and the U.S. DOE, Office of Science, Office of Advanced Scientific Computing Research, under the Accelerated Research in Quantum Computing (ARQC) program. E. P. acknowledges support from Intel Corporation under the FEINMAN Program. N.Y.Y. acknowledges support from the U.S. Department of Energy, Office of Basic Energy Sciences, Materials Sciences and Engineering Division, under Contract No. DE-AC02-05-CH11231 within the High Coherence Multilayer Superconducting Structures for Large Scale Qubit Integration and Photonic Transduction Program (QISLBNL).

- 
- [1] S. Das, Y. Tang, Z. Hong, M. Gonçalves, M. McCarter, C. Klewe, K. Nguyen, F. Gómez-Ortiz, P. Shafer, E. Arenholz, *et al.*, *Nature* **568**, 368 (2019).
  - [2] V. Kozii, Z. Bi, and J. Ruhman, *Phys. Rev. X* **9**, 031046 (2019).
  - [3] P. A. Volkov, P. Chandra, and P. Coleman, “Superconductivity from energy fluctuations in dilute quantum critical polar metals,” (2021), [arXiv:2106.11295 \[cond-mat.supr-con\]](#).
  - [4] K. Dunnett, J.-X. Zhu, N. A. Spaldin, V. Juričić, and A. V. Balatsky, *Phys. Rev. Lett.* **122**, 057208 (2019).
  - [5] L. Tu, X. Wang, J. Wang, X. Meng, and J. Chu, *Advanced Electronic Materials* **4**, 1800231.
  - [6] H. Ishiura, *J Nanosci Nanotechnol* **12**, 7619 (2012).
  - [7] S. Manipatruni, D. E. Nikonov, C.-C. Lin, T. A. Gosavi, H. Liu, B. Prasad, Y.-L. Huang, E. Bonturim, R. Ramesh, and I. A. Young, *Nature* **565**, 35 (2019).
  - [8] S.-C. Chang, A. Naeemi, D. E. Nikonov, and A. Gerverman, *Phys. Rev. Applied* **7**, 024005 (2017).
  - [9] L. W. Martin and A. M. Rappe, *Nature Reviews Materials*, 16087 (2016).
  - [10] B. A. McCullian, A. M. Thabt, B. A. Gray, A. L. Melen-

- dez, M. S. Wolf, V. L. Safonov, D. V. Pelekhov, V. P. Bhallamudi, M. R. Page, and P. C. Hammel, *Nature Communications* **11**, 5229 (2020).
- [11] S. Polisetty, J. Zhou, J. Karthik, A. R. Damodaran, D. Chen, A. Scholl, L. W. Martin, and M. Holcomb, *Journal of Physics: Condensed Matter* **24**, 245902 (2012).
- [12] A. Gruverman, M. Alexe, and D. Meier, *Nature Communications* **10**, 1661 (2019).
- [13] G. Grübel, A. Madsen, and A. Robert, in *Soft Matter Characterization* (Springer Netherlands, 2008) pp. 953–995.
- [14] C. R. Winkler, M. L. Jablonski, A. R. Damodaran, K. Jambunathan, L. W. Martin, and M. L. Taheri, *Journal of Applied Physics* **112**, 052013 (2012).
- [15] J. Grigas, *Microwave Dielectric Spectroscopy of Ferroelectrics and Related Materials* (CRC Press, 2019).
- [16] E. Parsonnet, Y.-L. Huang, T. Gosavi, A. Qualls, D. Nikonov, C.-C. Lin, I. Young, J. Bokor, L. W. Martin, and R. Ramesh, *Phys. Rev. Lett.* **125**, 067601 (2020).
- [17] H. Takenaka, I. Grinberg, S. Liu, and A. M. Rappe, *Nature* **546**, 391 (2017).
- [18] C. L. Degen, F. Reinhard, and P. Cappellaro, *Reviews of Modern Physics* **89**, 035002 (2017), [arXiv:1611.02427 \[quant-ph\]](https://arxiv.org/abs/1611.02427).
- [19] M. S. Grinolds, S. Hong, P. Maletinsky, L. Luan, M. D. Lukin, R. L. Walsworth, and A. Yacoby, *Nat Phys* **9**, 215 (2013).
- [20] Y. Dovzhenko, F. Casola, S. Schlotter, T. Zhou, F. Büttner, R. Walsworth, G. Beach, and A. Yacoby, *Nature communications* **9**, 2712 (2018).
- [21] S. Hsieh, P. Bhattacharyya, C. Zu, T. Mittiga, T. Smart, F. Machado, B. Kobrin, T. Höhn, N. Rui, M. Kamrani, *et al.*, *Science* **366**, 1349 (2019).
- [22] M. Block, B. Kobrin, A. Jarmola, S. Hsieh, C. Zu, N. L. Figueroa, V. M. Acosta, J. Minguzzi, J. R. Maze, D. Budker, and N. Y. Yao, “Optically enhanced electric field sensing using nitrogen-vacancy ensembles,” (2020), [arXiv:2004.02886 \[quant-ph\]](https://arxiv.org/abs/2004.02886).
- [23] T. Mittiga, S. Hsieh, C. Zu, B. Kobrin, F. Machado, P. Bhattacharyya, N. Rui, A. Jarmola, S. Choi, D. Budker, and *et al.*, *Physical Review Letters* **121** (2018).
- [24] S. Kolkowitz, A. Safira, A. High, R. Devlin, S. Choi, Q. Unterreithmeier, D. Patterson, A. Zibrov, V. Manucharyan, H. Park, *et al.*, *Science* **347**, 1129 (2015).
- [25] F. Casola, T. van der Sar, and A. Yacoby, *Nature Reviews Materials* **3**, 17088 (2018), [arXiv:1804.08742 \[cond-mat.str-el\]](https://arxiv.org/abs/1804.08742).
- [26] K. Agarwal, R. Schmidt, B. Halperin, V. Oganessian, G. Zaránd, M. D. Lukin, and E. Demler, *Phys. Rev. B* **95**, 155107 (2017).
- [27] J. F. Rodriguez-Nieva, K. Agarwal, T. Giamarchi, B. I. Halperin, M. D. Lukin, and E. Demler, *Phys. Rev. B* **98**, 195433 (2018).
- [28] A. Finco, A. Haykal, R. Tanos, F. Fabre, S. Chouaieb, W. Akhtar, I. Robert-Philip, W. Legrand, F. Ajejas, K. Bouzehouane, N. Reyren, T. Devolder, J.-P. Adam, J.-V. Kim, V. Cros, and V. Jacques, *Nature Communications* **12**, 767 (2021).
- [29] E. Schäfer-Nolte, L. Schlipf, M. Ternes, F. Reinhard, K. Kern, and J. Wrachtrup, *Phys. Rev. Lett.* **113**, 217204 (2014).
- [30] C. Li, M. Chen, D. Lyzwa, and P. Cappellaro, *Nano Letters* **19**, 7342 (2019), pMID: 31549847, <https://doi.org/10.1021/acs.nanolett.9b02960>.
- [31] D. Schmid-Lorch, T. Häberle, F. Reinhard, A. Zappe, M. Slota, L. Bogani, A. Finkler, and J. Wrachtrup, *Nano Letters* **15**, 4942 (2015), pMID: 26218205, <https://doi.org/10.1021/acs.nanolett.5b00679>.
- [32] A. Ariyaratne, D. Bluvstein, B. A. Myers, and A. C. B. Jayich, *Nature Communications* **9**, 2406 (2018).
- [33] S. Steinert, F. Ziem, L. T. Hall, A. Zappe, M. Schweikert, N. Götz, A. Aird, G. Balasubramanian, L. Hollenberg, and J. Wrachtrup, *Nature Communications* **4**, 1607 (2013).
- [34] A. Ermakova, G. Pramanik, J.-M. Cai, G. Algara-Siller, U. Kaiser, T. Weil, Y.-K. Tzeng, H. C. Chang, L. P. McGuinness, M. B. Plenio, B. Naydenov, and F. Jelezko, *Nano Letters* **13**, 3305 (2013), pMID: 23738579, <https://doi.org/10.1021/nl4015233>.
- [35] T. X. Zhou, J. J. Carmiggelt, L. M. Gächter, I. Esterlis, D. Sels, R. J. Stöhr, C. Du, D. Fernandez, J. F. Rodriguez-Nieva, F. Büttner, E. Demler, and A. Yacoby, *Proceedings of the National Academy of Sciences* **118** (2021), [10.1073/pnas.2019473118](https://doi.org/10.1073/pnas.2019473118).
- [36] B. A. McCullian, A. M. Thabt, B. A. Gray, A. L. Melen-dez, M. S. Wolf, V. L. Safonov, D. V. Pelekhov, V. P. Bhallamudi, M. R. Page, and P. C. Hammel, *Nature Communications* **11**, 5229 (2020).
- [37] J. F. Rodriguez-Nieva, D. Podolsky, and E. Demler, *arXiv e-prints*, [arXiv:1810.12333](https://arxiv.org/abs/1810.12333) (2018), [arXiv:1810.12333 \[cond-mat.mes-hall\]](https://arxiv.org/abs/1810.12333).
- [38] D. Prananto, Y. Kainuma, K. Hayashi, N. Mizuochi, K. ichi Uchida, and T. An, “Probing thermal magnon current mediated by coherent magnon via nitrogen-vacancy centers in diamond,” (2020), [arXiv:2007.13433](https://arxiv.org/abs/2007.13433).
- [39] H. Wang, S. Zhang, N. J. McLaughlin, B. Flebus, M. Huang, Y. Xiao, E. E. Fullerton, Y. Tserkovnyak, and C. R. Du, *arXiv e-prints*, [arXiv:2011.03905](https://arxiv.org/abs/2011.03905) (2020), [arXiv:2011.03905 \[cond-mat.mes-hall\]](https://arxiv.org/abs/2011.03905).
- [40] A. Rustagi, I. Bertelli, T. van der Sar, and P. Upadhyaya, *Phys. Rev. B* **102**, 220403 (2020), [arXiv:2009.05060 \[cond-mat.mes-hall\]](https://arxiv.org/abs/2009.05060).
- [41] H. Zhang, M. J. H. Ku, F. Casola, C. H. R. Du, T. van der Sar, M. C. Onbasli, C. A. Ross, Y. Tserkovnyak, A. Yacoby, and R. L. Walsworth, *Phys. Rev. B* **102**, 024404 (2020).
- [42] S. Chatterjee, J. F. Rodriguez-Nieva, and E. Demler, *Phys. Rev. B* **99**, 104425 (2019).
- [43] S. Chatterjee, P. E. Dolgirev, I. Esterlis, A. Zibrov, M. D. Lukin, N. Y. Yao, E. Demler, *et al.*, *arXiv preprint arXiv:2106.03859* (2021).
- [44] P. E. Dolgirev, S. Chatterjee, I. Esterlis, A. A. Zibrov, M. D. Lukin, N. Y. Yao, and E. Demler, *arXiv e-prints*, [arXiv:2106.05283](https://arxiv.org/abs/2106.05283) (2021), [arXiv:2106.05283 \[cond-mat.supr-con\]](https://arxiv.org/abs/2106.05283).
- [45] B. Flebus, H. Ochoa, P. Upadhyaya, and Y. Tserkovnyak, *Phys. Rev. B* **98**, 180409 (2018).
- [46] B. Flebus, *Phys. Rev. B* **100**, 064410 (2019).
- [47] N. J. McLaughlin, H. Wang, M. Huang, E. Lee-Wong, L. Hu, H. Lu, G. Q. Yan, G. Gu, C. Wu, Y.-Z. You, and C. R. Du, *Nano Letters* **21**, 7277–7283 (2021), pMID: 34415171.
- [48] S. Chatterjee, F. Machado, and N. Y. Yao, to appear.
- [49] We remark that, because we are interested in probing *near-equilibrium* dynamics, we do not depict time-

- resolution accessible via pump-probe techniques.
- [50] T. Astner, J. Gugler, A. Angerer, S. Wald, S. Putz, N. J. Mauser, M. Trupke, H. Sumiya, S. Onoda, J. Isoya, and et al., *Nature Materials* **17**, 313–317 (2018).
  - [51] D. M. Toyli, D. J. Christle, A. Alkauskas, B. B. Buckley, C. G. Van de Walle, and D. D. Awschalom, *Phys. Rev. X* **2**, 031001 (2012).
  - [52] G.-Q. Liu, X. Feng, N. Wang, Q. Li, and R.-B. Liu, *Nature communications* **10**, 1 (2019).
  - [53] To be precise, we write the retarded polarization correlation function as  $\chi_{\alpha\beta}(\mathbf{q}, \omega) = \hat{q}_\alpha \hat{q}_\beta \chi_L(\mathbf{q}, \omega) + (\delta_{\alpha\beta} - \hat{q}_\alpha \hat{q}_\beta) \chi_T(\mathbf{q}, \omega)$  and decompose the dielectric function as  $\varepsilon_{\alpha\beta}(\mathbf{q}, \omega) = \hat{q}_\alpha \hat{q}_\beta \varepsilon_L(\mathbf{q}, \omega) + (\delta_{\alpha\beta} - \hat{q}_\alpha \hat{q}_\beta) \varepsilon_T(\mathbf{q}, \omega)$ . Then  $\frac{\varepsilon_L(\mathbf{q}, \omega) - 1}{4\pi\varepsilon_L(\mathbf{q}, \omega)} = \chi_L(\mathbf{q}, \omega)$  and  $\frac{\varepsilon_T(\mathbf{q}, \omega) - 1}{4\pi} = \chi_T(\mathbf{q}, \omega)$  [54, 55].
  - [54] J.-P. Hansen and I. R. McDonald, *Theory of simple liquids* (Elsevier, 1990).
  - [55] C. G. Gray and K. E. Gubbins, *Theory of Molecular Fluids: Volume 1: Fundamentals* (Oxford University Press, 1984).
  - [56] See supplementary material.
  - [57] We remark that, in principle, by changing the orientation of the qubit sensor, one can extract not only  $\mathcal{C}(\omega, \mathbf{q}) = \text{Im}[\chi_{+-}(\omega, \mathbf{q}) + \chi_{-+}(\omega, \mathbf{q}) + 4\chi_{zz}(\omega, \mathbf{q})]$ , but also  $\text{Im}[\chi_{+-}(\omega, \mathbf{q})]$ ,  $\text{Im}[\chi_{-+}(\omega, \mathbf{q})]$ , and  $\text{Im}[\chi_{zz}(\omega, \mathbf{q})]$  individually.
  - [58] B. A. Myers, A. Ariyaratne, and A. C. B. Jayich, *Phys. Rev. Lett.* **118**, 197201 (2017).
  - [59] J. D. Breeze, E. Salvadori, J. Sathian, N. M. Alford, and C. W. M. Kay, *Nature* **555**, 493 (2018).
  - [60] P. Maletinsky, S. Hong, M. S. Grinolds, B. Hausmann, M. D. Lukin, R. L. Walsworth, M. Loncar, and A. Yacoby, *Nature Nanotechnology* **7**, 320 (2012).
  - [61] S. Sachdev, *Handbook of Magnetism and Advanced Magnetic Materials* (2007).
  - [62] E. L. Pollock and B. J. Alder, *Phys. Rev. Lett.* **46**, 950 (1981).
  - [63] G. Ascarelli, *Chemical Physics Letters* **39**, 23 (1976).
  - [64] A. Chandra and B. Bagchi, *The Journal of chemical physics* **92**, 6833 (1990).
  - [65] We remark that this expression is only valid in the case of an isotropic dispersion but has been generalized in the supplementary material.
  - [66] L. Pálková, P. Chandra, and P. Coleman, *Phys. Rev. B* **79**, 075101 (2009).
  - [67] L. M. Blinov, V. M. Fridkin, S. P. Palto, A. Bune, P. A. Dowben, and S. Ducharme, *Physics-Uspekhi* **43**, 243 (2000).
  - [68] A. J. Healey, A. Stacey, B. C. Johnson, D. A. Broadway, T. Teraji, D. A. Simpson, J.-P. Tetienne, and L. C. L. Hollenberg, *Phys. Rev. Materials* **4**, 104605 (2020).
  - [69] S. L. Sondhi, S. M. Girvin, J. P. Carini, and D. Shahar, *Rev. Mod. Phys.* **69**, 315 (1997).
  - [70] B. I. Halperin and P. C. Hohenberg, *Phys. Rev.* **177**, 952 (1969).
  - [71] B. I. Halperin, P. C. Hohenberg, and S.-k. Ma, *Phys. Rev. B* **10**, 139 (1974).
  - [72] B. I. Halperin, P. C. Hohenberg, and S.-k. Ma, *Phys. Rev. B* **13**, 4119 (1976).
  - [73] P. C. Hohenberg and B. I. Halperin, *Rev. Mod. Phys.* **49**, 435 (1977).
  - [74] S. Sachdev, *Nuclear Physics B* **464**, 576 (1996), [arXiv:cond-mat/9509147](https://arxiv.org/abs/cond-mat/9509147) [cond-mat].
  - [75] Y. Imry and S.-k. Ma, *Phys. Rev. Lett.* **35**, 1399 (1975).
  - [76] L. E. Cross, *Ferroelectrics* **76**, 241 (1987).
  - [77] G. Smolensky, *Ferroelectrics* **53**, 129 (1984).
  - [78] R. Cohen, *Nature* **441**, 941 (2006).
  - [79] R. Cowley, S. Gvasaliya, S. Lushnikov, B. Roessli, and G. Rotaru, *Advances in Physics* **60**, 229 (2011).
  - [80] G. G. G. Verri, *Theory of Relaxor Ferroelectrics* (University of California, Riverside, 2012).
  - [81] G. G. Guzmán-Verri, P. B. Littlewood, and C. M. Varma, *Phys. Rev. B* **88**, 134106 (2013).
  - [82] G. G. Guzmán-Verri and C. M. Varma, *Phys. Rev. B* **91**, 144105 (2015).
  - [83] Although such a model is known to be unable to capture the complex Vogel-Fuchler dynamics known to be associated with relaxor ferroelectrics, it has been shown to reproduce experimental measurements of the static structure factor.
  - [84] Y. Yafet, J. Kwo, and E. M. Gyorgy, *Phys. Rev. B* **33**, 6519 (1986).
  - [85] R. P. Erickson, *Phys. Rev. B* **46**, 14194 (1992).
  - [86] I.-K. Jeong, T. W. Darling, J. K. Lee, T. Proffen, R. H. Heffner, J. S. Park, K. S. Hong, W. Dmowski, and T. Egami, *Phys. Rev. Lett.* **94**, 147602 (2005).
  - [87] M. Paściak, T. Welberry, J. Kulda, M. Kempa, and J. Hlinka, *Physical Review B* **85**, 224109 (2012).
  - [88] M. Eremenko, V. Krayzman, A. Bosak, H. Playford, K. Chapman, J. Woicik, B. Ravel, and I. Levin, *Nature communications* **10**, 1 (2019).
  - [89] J. R. Maze, A. Gali, E. Togan, Y. Chu, A. Trifonov, E. Kaxiras, and M. D. Lukin, *New Journal of Physics* **13**, 025025 (2011).
  - [90] M. W. Doherty, N. B. Manson, P. Delaney, F. Jelezko, J. Wrachtrup, and L. C. Hollenberg, *Physics Reports* **528**, 1 (2013), the nitrogen-vacancy colour centre in diamond.
  - [91] E. Van Oort and M. Glasbeek, *Chemical Physics Letters* **168**, 529 (1990).
  - [92] While most previous reports focus on relaxation between the  $|m_s = 0\rangle \iff |m_s = \pm 1\rangle$  states, we note that our protocol is also affected by relaxation between  $|m_s = +1\rangle \iff |m_s = -1\rangle$  states which has been shown to be significant near surfaces [58].
  - [93] W. Zhong, R. King-Smith, and D. Vanderbilt, *Physical review letters* **72**, 3618 (1994).
  - [94] A. Jain, S. P. Ong, G. Hautier, W. Chen, W. D. Richards, S. Dacek, S. Cholia, D. Gunter, D. Skinner, G. Ceder, and K. a. Persson, *APL Materials* **1**, 011002 (2013).
  - [95] Y. Yamada and G. Shirane, *Journal of the Physical Society of Japan* **26**, 396 (1969), <https://doi.org/10.1143/JPSJ.26.396>.
  - [96] P. Yudin, J. Duchon, O. Pachterova, M. Klementova, T. Kocourek, A. Dejneka, and M. Tyunina, *Phys. Rev. Research* **3**, 033213 (2021).
  - [97] T. F. Nova, A. S. Disa, M. Fechner, and A. Cavalleri, *Science* **364**, 1075 (2019).
  - [98] J. Z. Zhao, L. C. Chen, B. Xu, B. B. Zheng, J. Fan, and H. Xu, *Phys. Rev. B* **101**, 121407 (2020).
  - [99] R. Kretschmer and K. Binder, *Phys. Rev. B* **20**, 1065 (1979).
  - [100] Z. Zheng, Q. Ma, Z. Bi, S. de la Barrera, M.-H. Liu, N. Mao, Y. Zhang, N. Kiper, K. Watanabe, T. Taniguchi, et al., *Nature* **588**, 71 (2020).
  - [101] K. Yasuda, X. Wang, K. Watanabe, T. Taniguchi, and P. Jarillo-Herrero, *Science* **372**, 1458–1462 (2021).

# Supplemental Material: Noise Electrometry of Polar and Dielectric Materials

Rahul Sahay,<sup>1,2</sup> Satcher Hsieh,<sup>2,3</sup> Eric Parsonnet,<sup>2</sup> Lane W. Martin,<sup>3,4</sup>  
Ramamoorthy Ramesh,<sup>2,3,4</sup> Norman Y. Yao,<sup>2,3</sup> and Shubhayu Chatterjee<sup>2</sup>

<sup>1</sup>*Department of Physics, Harvard University, Cambridge, Massachusetts 02138, USA*

<sup>2</sup>*Department of Physics, University of California, Berkeley, California 94720, USA*

<sup>3</sup>*Materials Sciences Division, Lawrence Berkeley National Laboratory, Berkeley, California 94720, USA*

<sup>4</sup>*Department of Materials Science and Engineering,  
University of California, Berkeley, California 94720, USA*

## DERIVATION OF QUBIT RELAXATION RATE

In this section, we systematically derive the relaxation rate of an impurity qubit sensor proximate to a polar or dielectric material in both a general setting and specific settings of interest. We start by deriving a relationship between the relaxation rate of the qubit and electrical noise at its location. Subsequently, we utilize Maxwell's equations to connect this electrical noise to polarization correlations in the nearby material. After this, we express the form of  $1/T_1$  in a number of settings of interest. Finally, we investigate the influence of magnetic noise for the specific case of the NV qubit.

### Impurity Qubit Response to Electrical Noise

Recall that in the main text, we defined the impurity qubit's coupling to electric and magnetic fields as (setting  $\hbar = 1$  henceforth):

$$H = H_0 + H_{q-EM} = \frac{\omega_q}{2} \sigma^z + \hat{\mathbf{d}} \cdot \mathbf{E} + \hat{\boldsymbol{\mu}} \cdot \mathbf{B}, \quad \hat{\mathbf{d}} = d_{\perp}(\sigma^x, \sigma^y, 0) \text{ and } \hat{\boldsymbol{\mu}} = \mu_z(0, 0, \sigma^z) \quad (\text{S1})$$

where  $d_{\perp}$  was the electrical dipole moment,  $\mu_z$  is the magnetic moment, and we assume that the quantization axis of the qubit is aligned with the physical  $z$ -axis of the system, defined as the axis normal to the plane of a proximate material. We assume that our sample is in thermal equilibrium at inverse temperature  $\beta$  with density matrix  $\rho = \frac{1}{Z} \sum_n e^{-\beta \varepsilon_n} |n\rangle \langle n|$ , where  $|n\rangle$  is an eigenstate of the sample at energy  $\varepsilon_n$  and  $Z = \sum_n e^{-\beta \varepsilon_n}$  is the partition function. Now, we use Fermi's golden rule to compute the transition rate between  $|1\rangle$  to  $|0\rangle$  (we set  $\hbar = 1$  and  $k_B = 1$  henceforth):

$$\Gamma_{em} = 2\pi d_{\perp}^2 \sum_{nm} \frac{e^{-\beta \varepsilon_n}}{Z} |\langle m, 0 | E^x \sigma^x + E^y \sigma^y | n, 1 \rangle|^2 \delta(\omega_q - (\varepsilon_m - \varepsilon_n)) \quad (\text{S2})$$

$$= 2\pi d_{\perp}^2 \sum_{nm} \frac{e^{-\beta \varepsilon_n}}{Z} |\langle m, 0 | E^x + iE^y | n, 0 \rangle|^2 \delta(\omega_q - (\varepsilon_m - \varepsilon_n)) \quad (\text{S3})$$

$$= 2\pi d_{\perp}^2 \sum_{nm} \frac{e^{-\beta \varepsilon_n}}{Z} E_{mn}^+ E_{nm}^- \delta(\omega_q - (\varepsilon_m - \varepsilon_n)) \quad (\text{S4})$$

where the argument of the delta enforces energy conservation, i.e, the amount of energy lost by the qubit ( $\omega_q = E_1 - E_0$ ) equals the amount of energy gained by the sample ( $\varepsilon_m - \varepsilon_n$ ). Similarly, we have that:

$$\Gamma_{abs} = 2\pi d_{\perp}^2 \sum_{nm} \frac{e^{-\beta \varepsilon_n}}{Z} E_{mn}^- E_{nm}^+ \delta(\omega_q + (\varepsilon_m - \varepsilon_n)) \quad (\text{S5})$$

where  $E^{\pm} = E_x \pm iE_y$ . Thus, we can write  $1/T_1 = 1/2(\Gamma_{abs} + \Gamma_{em})$  [1]. Now, to relate this quantity to the electric field fluctuations, note that the noise tensor is given by:

$$\mathcal{N}_{ij}(\omega) = \frac{1}{2} \int_{-\infty}^{\infty} dt \langle \{E^i(t), E^j(0)\} \rangle e^{i\omega t} = \pi \sum_{nm} \frac{e^{-\beta \varepsilon_n}}{Z} [E_{nm}^i E_{mn}^j \delta(\omega - (\varepsilon_m - \varepsilon_n)) + E_{nm}^j E_{mn}^i \delta(\omega - (\varepsilon_n - \varepsilon_m))] \quad (\text{S6})$$



Thus, it follows that:

$$\frac{1}{T_1} = d_{\perp}^2 \mathcal{N}_{-+}(\omega_q) \quad (\text{S7})$$

Subsequently, by the fluctuation-dissipation theorem

$$\mathcal{N}_{ij}(\omega) = \frac{1}{2} \coth\left(\frac{\beta\omega}{2}\right) \mathcal{S}_{ij}(\omega) \text{ where } \mathcal{S}_{ij}(\omega) = \int_{-\infty}^{\infty} dt \langle [E^i(t), E^j(0)] \rangle e^{i\omega t} \quad (\text{S8})$$

Moreover, we can relate  $\mathcal{S}_{ij}(\omega)$  in terms of the retarded correlators of the electric field, which are more convenient to calculate

$$\mathcal{S}_{ij}(\omega) = 2 \text{Im} [C_{E^i E^j}^R(\omega)] \text{ where } C_{E^i E^j}^R(\omega) = i \int_{-\infty}^{\infty} dt \Theta(t) \langle [E^i(t), E^j(0)] \rangle e^{i\omega t} \quad (\text{S9})$$

### Propagation of Maxwell's Equations

To determine the electrical noise arising from dipolar fluctuations, we propagate these fluctuations using Maxwell's equations in Lorentz gauge:

$$\partial^2 A^\mu(\mathbf{r}, t) = \mu_0 J^\mu(\mathbf{r}, t) = \mu_0 \begin{pmatrix} -c \nabla \cdot \mathbf{P}(\mathbf{r}, t) + c \sigma(\mathbf{r}, t) \\ \partial_t \mathbf{P}(\mathbf{r}, t) \end{pmatrix} \quad (\text{S10})$$

where  $\partial^2 = -\partial_t^2/c^2 + \nabla^2$ ,  $\mathbf{P}(\mathbf{r}, t) = \mathbf{P}(\mathbf{r}, t) 1_{[-w, 0]}(z)$  (where  $1_{[-w, 0]}$  is 1 for  $z \in [-w, 0]$  and 0 otherwise),  $\sigma(\mathbf{r}, t) = P_z(\mathbf{r}, t) \delta(z) - P_z(\mathbf{r}, t) \delta(z + w)$  is the surface charge density, and  $w$  is the width of the sample. We can solve these equations by introducing a kernel  $G_i^\mu(\mathbf{r}, \mathbf{r}', t - t')$ :

$$A^\mu(\mathbf{r}, t) = \mu_0 \int_{-\infty}^{\infty} dt' d^3 \mathbf{r}' G_i^\mu(\mathbf{r}, \mathbf{r}', t - t') P_i(\mathbf{r}', t') \quad (\text{S11})$$

where  $i$  labels  $x, y, z$  and we are implicitly summing over repeated indices. We define  $G_i^\mu$  to satisfy the equation:

$$\partial^2 G_i^\mu(\rho - \rho', z, z', t - t') = \begin{pmatrix} c \delta(t - t') \partial_i [\delta^{(3)}(\mathbf{r} - \mathbf{r}')] + c \delta_{i,z} \delta^{(3)}(\mathbf{r} - \mathbf{r}') [\delta(z) - \delta(z + w)] \\ - \delta^{(3)}(\mathbf{r} - \mathbf{r}') \partial_t [\delta(t - t')] \hat{e}_i \end{pmatrix} \quad (\text{S12})$$

where  $\rho = (x, y)$  is the coordinates of the material in-plane. Now, to solve for  $G_i^\mu$ , we can express  $A^\mu, G_i^\mu$ , and our polarization  $P_i$  in terms of their in-plane Fourier modes yielding:

$$A^\mu(\mathbf{r}, t) = \frac{1}{\sqrt{L^2}} \sum_{\mathbf{q}} \int \frac{d\omega}{2\pi} A^\mu(z, \mathbf{q}, \omega) e^{i(\mathbf{q} \cdot \rho - \omega t)} \quad (\text{S13})$$

$$G_i^\mu(\rho, z, z', t) = \frac{1}{L^2} \sum_{\mathbf{q}} \int \frac{d\omega}{2\pi} G_i^\mu(z, z', \mathbf{q}, \omega) e^{i(\mathbf{q} \cdot \rho - \omega t)} \quad (\text{S14})$$

$$P_i(\mathbf{r}, t) = \frac{1}{\sqrt{L^2}} \sum_{\mathbf{q}} \int \frac{d\omega}{2\pi} P_i(z, \mathbf{q}, \omega) e^{i(\mathbf{q} \cdot \rho - \omega t)} \quad (\text{S15})$$

where we assumed a sample with transverse dimensions  $L \times L$  for simplicity. When we plug this back into the equations of motion for  $G_i^\mu$ , we get:

$$(-\lambda^2 + \partial_z^2) G_i^\mu(z, z', \mathbf{q}, \omega) = \begin{pmatrix} i c q_i (\delta_{i,x} + \delta_{i,y}) \delta(z - z') + c \delta_{i,z} \partial_z [\delta(z - z')] + c \delta_{i,z} \delta(z - z') [\delta(z) - \delta(z + w)] \\ i \omega \delta(z - z') \hat{e}_i \end{pmatrix} \quad (\text{S16})$$

where  $\lambda^2 = (q^2 - \omega^2/c^2)$ . To solve this, we Fourier transform the  $z$  coordinate as

$$G_i^\mu(\alpha, z', \mathbf{q}, \omega) = \int dz e^{-i\alpha z} G_i^\mu(z, z', \mathbf{q}, \omega) \quad (\text{S17})$$

and so we get the following:

$$G_i^\mu(\alpha, z', \mathbf{q}, \omega) = -\frac{1}{\lambda^2 + \alpha^2} \left( \frac{icq_i(\delta_{i,x} + \delta_{i,y})e^{-i\alpha z'} + ic\delta_{i,z}\alpha e^{-i\alpha z'} + c\delta_{i,z} \int dz e^{-i\alpha z} \delta(z - z') [\delta(z) - \delta(z + w)]}{i\omega e^{-i\alpha z'} \hat{e}_i} \right) \quad (\text{S18})$$

Now, we Fourier transform back to get a useable expression for  $G$ . We do this one component at a time:

$$G_i^0 = -\frac{icq_i(\delta_{i,x} + \delta_{i,y})}{2\lambda} e^{-\lambda|z-z'|} - \frac{c\delta_{i,z}}{2} \text{sgn}(z - z') e^{-\lambda|z-z'|} - c\delta_{i,z} \int \frac{d\alpha d\tilde{z}}{2\pi} \frac{e^{i\alpha(z-\tilde{z})} \delta(\tilde{z} - z') [\delta(\tilde{z}) - \delta(\tilde{z} + w)]}{\lambda^2 + \alpha^2} \quad (\text{S19})$$

$$= -\frac{icq_i(\delta_{i,x} + \delta_{i,y})}{2\lambda} e^{-\lambda|z-z'|} - \frac{c\delta_{i,z}}{2} \text{sgn}(z - z') e^{-\lambda|z-z'|} - c\delta_{i,z} \int d\tilde{z} \frac{e^{-\lambda|z-\tilde{z}|}}{2\lambda} \delta(\tilde{z} - z') [\delta(\tilde{z}) - \delta(\tilde{z} + w)] \quad (\text{S20})$$

$$= -\frac{icq_i(\delta_{i,x} + \delta_{i,y})}{2\lambda} e^{-\lambda|z-z'|} - \frac{c\delta_{i,z}}{2} \text{sgn}(z - z') e^{-\lambda|z-z'|} - \frac{c\delta_{i,z} e^{-\lambda|z-z'|}}{2\lambda} [\delta(z') - \delta(z' + w)] \quad (\text{S21})$$

Also, we have that:

$$G_i^j = -i\omega \frac{e^{-\lambda|z-z'|}}{2\lambda} \delta_i^j \quad (\text{S22})$$

where  $i, j \in \{x, y, z\}$ . Now, we can decompose our Green's function as:

$$G_i^\mu(z, z', \mathbf{q}, \omega) = \mathcal{G}_i^\mu(z - z', \mathbf{q}, \omega) + g_i^\mu(z, z', \mathbf{q}, \omega) \quad (\text{S23})$$

where

$$\mathcal{G}_i^\mu(z - z', \mathbf{q}, \omega) = \begin{pmatrix} -\frac{icq_i(\delta_{i,x} + \delta_{i,y})}{2\lambda} e^{-\lambda|z-z'|} - \frac{c\delta_{i,z}}{2} \text{sgn}(z - z') e^{-\lambda|z-z'|} \\ -i\omega \frac{e^{-\lambda|z-z'|}}{2\lambda} \hat{e}_i \end{pmatrix} \quad (\text{S24})$$

$$g_i^\mu = \begin{pmatrix} -\frac{c\delta_{i,z} e^{-\lambda|z-z'|}}{2\lambda} [\delta(z') - \delta(z' + w)] \\ 0 \end{pmatrix} \quad (\text{S25})$$

indicate bulk and surface terms respectively. Green's function in hand, we can relate the polarization back to the vector potential as:

$$A^\mu(\mathbf{r}, t) = \frac{\mu_0}{L} \sum_{\mathbf{q}} \int \frac{dz' d\omega}{2\pi} G_i^\mu(z, z', \mathbf{q}, \omega) P_i(z', \mathbf{q}, \omega) e^{i(\mathbf{q} \cdot \mathbf{r} - \omega t)} \quad (\text{S26})$$

$$= \frac{1}{L} \sum_{\mathbf{q}} \int \frac{dz' d\omega}{2\pi} \mathcal{G}_i^\mu(|z - z'|, \mathbf{q}, \omega) P_i(z, \mathbf{q}, \omega) e^{i(\mathbf{q} \cdot \mathbf{r} - \omega t)} + \frac{1}{L} \sum_{\mathbf{q}} \int \frac{dz' d\omega}{2\pi} g_i^\mu(z, z', \mathbf{q}, \omega) P_i(z', \mathbf{q}, \omega) e^{i(\mathbf{q} \cdot \mathbf{r} - \omega t)} \quad (\text{S27})$$

Therefore, we can compute the electric field as:

$$\mathbf{E}(\mathbf{r}, t) = -c\nabla A^0(\mathbf{r}, t) - \partial_t \mathbf{A}(\mathbf{r}, t) = \frac{\mu_0}{L} \sum_{\mathbf{q}} \int \frac{d\omega dz'}{2\pi} \mathbf{H}_i(z, z', \mathbf{q}, \omega) P_i(z', \mathbf{q}, \omega) e^{i(\mathbf{q} \cdot \mathbf{r} - \omega t)} \quad (\text{S28})$$

where

$$\mathbf{H}_i = \begin{pmatrix} -icq_x G_i^0 + i\omega G_i^x \\ -icq_y G_i^0 + i\omega G_i^y \\ -c\partial_z G_i^0 + i\omega G_i^z \end{pmatrix} = \mathcal{H}_i + \mathbf{h}_i \quad (\text{S29})$$

For reference, the explicit form of the bulk kernels is:

$$\mathcal{H}_x = -\frac{e^{-\lambda|z-z'|}}{2\lambda} \begin{pmatrix} c^2 q_x^2 + \omega^2 \\ c^2 q_x q_y \\ ic^2 q_x \lambda \cdot \text{sign}(z - z') \end{pmatrix} \quad \mathcal{H}_y = -\frac{e^{-\lambda|z-z'|}}{2\lambda} \begin{pmatrix} c^2 q_x q_y \\ c^2 q_y^2 + \omega^2 \\ ic^2 q_y \lambda \cdot \text{sign}(z - z') \end{pmatrix} \quad (\text{S30})$$

$$\mathcal{H}_z = -\frac{e^{-\lambda|z-z'|}}{2} \begin{pmatrix} -ic^2 q_x \text{sign}(z - z') \\ -ic^2 q_y \text{sign}(z - z') \\ -c^2 \delta(z - z') + \frac{c^2 \lambda^2 \text{sign}(z - z') + \omega^2}{\lambda} \end{pmatrix} \quad (\text{S31})$$

and the explicit form of the surface kernels are:

$$\mathbf{h}_z = \frac{c^2 e^{-\lambda|z-z'|}}{2\lambda} \begin{pmatrix} iq_x \\ iq_y \\ -\partial_z \end{pmatrix} [\delta(z') - \delta(z' + w)] = \frac{c^2 e^{-\lambda|z-z'|}}{2\lambda} \begin{pmatrix} iq_x \\ iq_y \\ -\partial_z \end{pmatrix} \mathcal{S}(z') \quad (\text{S32})$$

with  $\mathbf{h}_{x,y} = 0$ .

### Qubit Relaxation from Dipolar Fluctuations (Translation Invariant)

Having propagated the in-sample polarization to the electric fields outside of the material, we now determine the relaxation rate of our probe qubit due to in-sample polarization fluctuations. To do so, we compute electrical noise at the location of the probe qubit due to these fluctuations. In particular, by Eq. S7 and S8, we need to compute:

$$\langle [E_-(\mathbf{r}, t), E_+(\mathbf{r}, 0)] \rangle = \frac{\mu_0^2}{L^2} \sum_{\mathbf{q}_1, \mathbf{q}_2} \int \frac{d\omega_1 d\omega_2 dz'_1 dz'_2}{(2\pi)^2} H_i^-(z'_1, \mathbf{q}_1, \omega_1) H_j^+(z'_2, \mathbf{q}_2, \omega_2) \quad (\text{S33})$$

$$\times \langle [P_i(z'_1, \mathbf{q}_1, \omega_1), P_j(z'_2, \mathbf{q}_2, \omega_2)] \rangle e^{i(\mathbf{q}_1 \cdot \boldsymbol{\rho} - \omega_1 t)} e^{i\mathbf{q}_2 \cdot \boldsymbol{\rho}} \quad (\text{S34})$$

where  $\mathbf{r} = (\rho, d) = (0, 0, d)$  is the location of the qubit. Assuming spacetime translation invariance, we have that

$$\langle [P_i(z'_1, \mathbf{q}_1, \omega_1), P_j(z'_2, \mathbf{q}_2, \omega_2)] \rangle = 2\pi \delta(\omega_1 + \omega_2) \delta_{\mathbf{q}_1, -\mathbf{q}_2} \langle [P_i(z'_1, \mathbf{q}, \omega), P_j(z'_2, -\mathbf{q}, -\omega)] \rangle \quad (\text{S35})$$

Thus, the electrical noise can be expressed as:

$$\langle [E_-(\mathbf{r}, t), E_+(\mathbf{r}, 0)] \rangle = \frac{\mu_0^2}{L^2} \sum_{\mathbf{q}} \int \frac{d\omega dz'_1 dz'_2}{2\pi} H_i^-(z'_1, \mathbf{q}, \omega) H_j^-(z'_2, -\mathbf{q}, -\omega) \langle [P_i(z'_1, \mathbf{q}, \omega), P_j(z'_2, -\mathbf{q}, -\omega)] \rangle e^{-i\omega t} \quad (\text{S36})$$

To proceed further, we simply need to contract the product of kernels with the polarization commutator:

$$H_i^-(1) H_j^+(2) \langle [P_i(1), P_j(1)] \rangle = \left\langle \left[ \frac{1}{2} (H_+^-(1) P_-(1) + H_-^-(1) P_+(1)) + H_z^-(1) P_z(1), \right. \right. \quad (\text{S37})$$

$$\left. \frac{1}{2} (H_+^+(2) P_-(2) + H_-^+(2) P_+(2)) + H_z^+(2) P_z(2) \right] \rangle \quad (\text{S38})$$

$$= \frac{1}{4} (H_+^-(1) H_+^+(2) \langle [P_-(1), P_+(2)] \rangle + H_-^-(1) H_+^+(2) \langle [P_+(1), P_-(2)] \rangle + H_z^-(1) H_z^+(2) \langle [P_z(1), P_z(2)] \rangle) \quad (\text{S39})$$

$$+ \frac{1}{4} (H_+^-(1) H_+^+(2) \langle [P_-(1), P_-(2)] \rangle + H_-^-(1) H_+^+(2) \langle [P_+(1), P_+(2)] \rangle) \quad (\text{S40})$$

$$+ \frac{1}{2} (H_+^-(1) H_z^+(2) \langle [P_-(1), P_z(2)] \rangle + H_-^-(1) H_z^+(2) \langle [P_+(1), P_z(2)] \rangle) \quad (\text{S41})$$

$$+ H_z^-(1) H_+^+(2) \langle [P_z(1), P_+(2)] \rangle + H_z^-(1) H_+^+(2) \langle [P_z(1), P_-(2)] \rangle) \quad (\text{S42})$$

where  $H_i^-(1) = H_i^-(d, z_1, \mathbf{q}_1, \omega_1)$ ,  $H_j^+(2) = H_j^+(d, z_2, \mathbf{q}_2, \omega'_2)$ ,  $P_i(1) = P_i(z_1, \mathbf{q}_1, \omega_1)$ , and  $P_j(2) = P_j(z_2, \mathbf{q}_2, \omega_2)$  with  $\mathbf{q}_1 = -\mathbf{q}_2 = \mathbf{q}$  and  $\omega_1 = -\omega_2 = \omega$  and also  $H_\pm^\pm = H_x^\pm \pm iH_y^\pm$  and  $P_\pm = P_x \pm iP_y$ . Although the above expression looks daunting, the first line is the only line that appreciably contributes when either it is a good approximation that the polarization is conserved or when the sample is rotationally invariant. Now we compute the product of the kernels in the approximation that  $\omega/c \ll q$  (i.e. the speed of light is much faster than any velocity scale in the material). We remark that:

$$H_+^+ = -\frac{e^{-\lambda|z-z'|}}{2\lambda} c^2 (q_x + iq_y)^2 \quad H_-^- = -\frac{e^{-\lambda|z-z'|}}{2\lambda} (q_x - iq_y)^2 \quad H_-^+ = H_+^- = -\frac{e^{-\lambda|z-z'|}}{2\lambda} (c^2 q^2 + 2\omega^2) \quad (\text{S43})$$

$$H_z^\pm = \frac{e^{-\lambda|z-z'|}}{2\lambda} ic^2 (q_x \pm iq_y) [\lambda \cdot \text{sign}(z - z') + \mathcal{S}(z')] \quad (\text{S44})$$

Now, we can compute the products of these kernels. First, the polarization conserving kernels:

$$H_-^-(1) H_+^+(2) \approx \frac{1}{4} e^{-q|z-z'_1|} e^{-q|z-z'_2|} c^4 q^2 = F(z, q; z'_1, z'_2) \quad (\text{S45})$$

$$H_+^-(1) H_-^+(2) \approx \frac{1}{4} e^{-q|z-z'_1|} e^{-q|z-z'_2|} c^4 q^2 = F(z, q; z'_1, z'_2) \quad (\text{S46})$$

and also

$$H_z^-(1)H_z^+(2) \approx \frac{1}{4}e^{-q|z-z'_1|}e^{-q|z-z'_2|}c^4(q^2 + q(\mathcal{S}(z'_1) + \mathcal{S}(z'_2)) + \mathcal{S}(z'_1)\mathcal{S}(z'_2)) \quad (\text{S47})$$

$$= F(z, q; z'_1, z'_2) \left[ 1 + \frac{1}{q}(\mathcal{S}(z'_1) + \mathcal{S}(z'_2)) + \frac{1}{q^2}\mathcal{S}(z'_1)\mathcal{S}(z'_2) \right] \quad (\text{S48})$$

Now, the other terms:

$$H_+^-(1)H_+^+(2) \approx \frac{1}{4}e^{-q|z-z'_1|}e^{-q|z-z'_2|}c^4q^2e^{2i\varphi} = F(z, q; z'_1, z'_2)e^{2i\varphi} \quad (\text{S49})$$

$$H_-^-(1)H_-^+(2) \approx \frac{1}{4}e^{-q|z-z'_1|}e^{-q|z-z'_2|}c^4q^2e^{-2i\varphi} = F(z, q; z'_1, z'_2)e^{-2i\varphi} \quad (\text{S50})$$

$$H_+^-(1)H_z^+(2) \approx -\frac{1}{4}e^{-q|z-z'_1|}e^{-q|z-z'_2|}(-ie^{i\varphi})c^4[q^2 + q\mathcal{S}(z'_2)] = ie^{i\varphi}F(z, q; z'_1, z'_2) \left[ 1 + \frac{1}{q}\mathcal{S}(z'_2) \right] \quad (\text{S51})$$

$$H_-^-(1)H_z^+(2) \approx -\frac{1}{4}e^{-q|z-z'_1|}e^{-q|z-z'_2|}(-ie^{-i\varphi})c^4[q^2 + q\mathcal{S}(z'_2)] = ie^{-i\varphi}F(z, q; z'_1, z'_2) \left[ 1 + \frac{1}{q}\mathcal{S}(z'_2) \right] \quad (\text{S52})$$

$$H_z^-(1)H_+^+(2) \approx -\frac{1}{4}e^{-q|z-z'_1|}e^{-q|z-z'_2|}ie^{i\varphi}c^4[q^2 + q\mathcal{S}(z'_1)] = -ie^{i\varphi}F(z, q; z'_1, z'_2) \left[ 1 + \frac{1}{q}\mathcal{S}(z'_1) \right] \quad (\text{S53})$$

$$H_z^-(1)H_-^+(2) \approx -\frac{1}{4}e^{-q|z-z'_1|}e^{-q|z-z'_2|}ie^{-i\varphi}c^4[q^2 + q\mathcal{S}(z'_1)] = -ie^{-i\varphi}F(z, q; z'_1, z'_2) \left[ 1 + \frac{1}{q}\mathcal{S}(z'_1) \right] \quad (\text{S54})$$

where  $\varphi$  is the angle that  $\mathbf{q}$  makes in the  $xy$  plane. Now, we can write the full expression for the electrical noise:

$$\langle [E_-(\mathbf{r}, t), E_+(\mathbf{r}, 0)] \rangle = \frac{\mu_0^2}{L^2} \sum_{\mathbf{q}} \int \frac{d\omega dz'_1 dz'_2}{2\pi} F(d, q; z'_1, z'_2) \times (\mathcal{C}_{bb} + \mathcal{C}_{bs} + \mathcal{C}_{ss}) e^{-i\omega t} \quad (\text{S55})$$

where  $\mathcal{C}_{bb}$  are bulk-bulk correlations,  $\mathcal{C}_{bs}$  are correlations between the bulk and the surface,  $\mathcal{C}_{ss}$  are correlations between the two surfaces of the sample. Let us enumerate these one-by-one:

$$\mathcal{C}_{bb} = \frac{1}{16} (\langle [P_+(1), P_-(2)] \rangle + \langle [P_-(1), P_+(2)] \rangle + 4\langle [P_z(1), P_z(2)] \rangle) \quad (\text{S56})$$

$$+ \frac{1}{16} (\langle [P_-(1), P_-(2)] \rangle e^{2i\varphi} + \langle [P_+(1), P_+(2)] \rangle e^{-2i\varphi}) \quad (\text{S57})$$

$$+ \frac{1}{8} [\langle [P_-(1), P_z(2)] \rangle ie^{i\varphi} + \langle [P_+(1), P_z(2)] \rangle ie^{-i\varphi} - (\langle [P_z(1), P_-(1)] \rangle ie^{i\varphi} + \langle [P_z(1), P_+(1)] \rangle ie^{-i\varphi})] \quad (\text{S58})$$

where the parenthesis in the last term indicate complex conjugate pairs. Moreover, we have that:

$$\mathcal{C}_{bs} = \frac{\mathcal{S}(z'_1)}{8q} (2\langle [P_z(1), P_z(2)] \rangle - ie^{i\varphi}\langle [P_z(1), P_-(2)] \rangle - ie^{-i\varphi}\langle [P_z(1), P_+(2)] \rangle) \quad (\text{S59})$$

$$+ \frac{\mathcal{S}(z'_2)}{8q} (2\langle [P_z(1), P_z(2)] \rangle + ie^{i\varphi}\langle [P_-(1), P_z(2)] \rangle + ie^{-i\varphi}\langle [P_+(1), P_z(2)] \rangle) \quad (\text{S60})$$

Finally, we have the surface-surface correlations:

$$\mathcal{C}_{ss} = \frac{1}{4q^2} \mathcal{S}(z'_1)\mathcal{S}(z'_2)\langle [P_z(1), P_z(2)] \rangle \quad (\text{S61})$$

So, we can write down our relaxation rate as:

$$\frac{1}{T_1} = \frac{1}{2} d_{\perp}^2 \coth\left(\frac{\beta\omega}{2}\right) \frac{\mu_0^2}{L^2} \sum_{\mathbf{q}} \int dz'_1 dz'_2 F(d, \mathbf{q}; z'_1, z'_2) \times \{\mathcal{C}_{bb} + \mathcal{C}_{bs} + \mathcal{C}_{ss}\} \quad (\text{S62})$$

Note that in the special case where the material is a stack of  $N$  2D layers each of width  $w$ , we can re-express our correlators as

$$\langle [P_{\alpha}(z'_1, \mathbf{q}, \omega), P_{\beta}(z'_2, -\mathbf{q}, -\omega)] \rangle = \sum_{j=0}^{N-1} \langle [P_{\alpha}(\mathbf{q}, \omega), P_{\beta}(-\mathbf{q}, -\omega)] \rangle \delta(z'_1 - jw) \delta(z'_2 - jw) \quad (\text{S63})$$



Consequently, the expression for  $1/T_1$  can be re-written as:

$$\frac{1}{T_1} = \frac{1}{2} d_\perp^2 \coth\left(\frac{\beta\omega_q}{2}\right) \frac{\mu_0^2}{L^2} \sum_{\mathbf{q}} F(d, \mathbf{q}) \times \{\mathcal{C}_{bb} + \mathcal{C}_{bs} + \mathcal{C}_{ss}\} \quad (\text{S64})$$

where  $F(d, \mathbf{q}) = \sum_{j=0}^{N-1} c^4 q^2 e^{-2q(d+jw)}$  and  $\mathcal{C}_{bb}, \mathcal{C}_{bs}$ , and  $\mathcal{C}_{ss}$  are redefined with  $\langle [P_\alpha(\mathbf{q}, \omega), P_\beta(-\mathbf{q}, -\omega)] \rangle$  instead of  $\langle [P_\alpha(z'_1, \mathbf{q}, \omega), P_\beta(z'_2, -\mathbf{q}, -\omega)] \rangle$ . If we neglect the surface charge contributions  $\mathcal{C}_{bs}, \mathcal{C}_{ss}$  and impose rotational invariance in-plane, this is precisely Eq. 3 of the main text.

### Influence of Magnetic Noise

In the main text, we quoted that the relative strength of  $1/T_1$  due to magnetic noise emanating from dipoles to electrical noise is controlled by  $\mu_z^2 c_s^2 / d_\perp^2 c^4 \sim 10^{-4} \ll 1$  for the nitrogen-vacancy center. In this section, we derive this.

Recall that the coupling of an NV center to magnetic fields is given by:

$$H_{NV-B} = \mu_z \mathbf{B} \cdot \mathbf{S} = \mu_z B_z S_z + \mu_z \frac{B_x}{2} (S_+ + S_-) - \mu_z \frac{iB_y}{2} (S_+ - S_-) = \mu_z \left( B_z S_z + \frac{1}{2} (B_- S_+ + B_+ S_-) \right) \quad (\text{S65})$$

where  $\mu_z = 2.8 \text{ MHz/G}$  and  $B_\pm = B_x \pm iB_y$ . We note that such a Hamiltonian is incapable of driving transitions between the  $|\pm 1\rangle$  states of the NV center because each term can only change the magnetic quantum number by at most one. Hence, magnetic field noise acts to enhance the decay rate between the  $|0\rangle$  and  $|\pm 1\rangle$  states of the NV center. To estimate this effect, we compute the decay rate from  $|+\rangle$  to  $|0\rangle$ , split by  $\omega$ :

$$\Gamma_{em} = \frac{\pi\mu_z^2}{2} \sum_{n,m} \frac{e^{-\beta\epsilon_n}}{Z} |\langle m, 0 | B_- S_+ + B_+ S_- | n, + \rangle|^2 \delta(\omega - \epsilon_m + \epsilon_n) \quad (\text{S66})$$

$$= \pi\mu_z^2 \sum_{n,m} \frac{e^{-\beta\epsilon_n}}{Z} |B_{mn}^+|^2 \delta(\omega - (\epsilon_m - \epsilon_n)) = \pi\mu_z^2 \sum_{n,m} \frac{e^{-\beta\epsilon_n}}{Z} B_{nm}^- B_{mn}^+ \delta(\omega - (\epsilon_m - \epsilon_n)) \quad (\text{S67})$$

Similarly,

$$\Gamma_{abs} = \pi\mu_z^2 \sum_{n,m} \frac{e^{-\beta\epsilon_n}}{Z} B_{nm}^+ B_{mn}^- \delta(\omega + (\epsilon_m - \epsilon_n)) \quad (\text{S68})$$

Now, the full expression for  $1/T_1 = \frac{1}{2} [\Gamma_{em} + \Gamma_{abs}]$  and can be written from the noise tensor because:

$$\mathcal{N}_{ij}(\omega) = \frac{1}{2} \int_{-\infty}^{\infty} dt \langle \{B^i(t), B^j(0)\} \rangle e^{i\omega t} = \pi \sum_{n,m} \frac{e^{-\beta\epsilon_n}}{Z} [B_{nm}^i B_{mn}^j \delta(\omega - (\epsilon_m - \epsilon_n)) + B_{nm}^j B_{mn}^i \delta(\omega + (\epsilon_m - \epsilon_n))] \quad (\text{S69})$$

Thus, we have in total:

$$\frac{1}{T_1} = \frac{\mu_z^2}{2} \mathcal{N}_{-+}(\omega) = \frac{\mu_z^2}{4} \coth\left(\frac{\beta\omega}{2}\right) \mathcal{S}_{-+}(\omega) = \frac{\mu_z^2}{4} \coth\left(\frac{\beta\omega}{2}\right) \int_{-\infty}^{\infty} dt \langle [B^-(t), B^+(0)] \rangle e^{i\omega t} \quad (\text{S70})$$

Expression in hand, we will now estimate the rough magnitude of the magnetic contribution to  $1/T_1$ . Note that we compute the magnetic field as:

$$\mathbf{B}(\mathbf{r}, t) = \nabla \times \mathbf{A}(\mathbf{r}, t) = \frac{\mu_0}{L} \sum_{\mathbf{q}} \int \frac{dz' d\omega}{2\pi} \mathbf{H}_i(z, z', \mathbf{q}, \omega) P_i(z', \mathbf{q}, \omega) e^{i(\mathbf{q} \cdot \rho - \omega t)} \quad (\text{S71})$$

where  $\mathbf{H}_i = \nabla \times (\mathbf{G}_i e^{i(\mathbf{q} \cdot \rho - \omega t)}) e^{-i(\mathbf{q} \cdot \rho - \omega t)} = \mathbf{H}_i + \mathbf{h}_i$  representing bulk and surface contributions. We can use Eqs. S24 and S25 to get:

$$\mathbf{H}_i = \begin{pmatrix} iq_y \mathcal{G}_i^z - \partial_z \mathcal{G}_i^y \\ \partial_z \mathcal{G}_i^x - iq_x \mathcal{G}_i^z \\ iq_x \mathcal{G}_i^y - iq_y \mathcal{G}_i^x \end{pmatrix} = \begin{pmatrix} -q_y \delta_{iz} + i\lambda \delta_{iy} \\ -i\lambda \delta_{ix} + q_x \delta_{iz} \\ -q_x \delta_{iy} + q_y \delta_{ix} \end{pmatrix} \frac{\omega}{2\lambda} e^{-\lambda|z-z'|} \quad (\text{S72})$$

and  $\mathbf{h}_i = 0$ .

Having propagated the in-sample polarization to the magnetic fields outside of the material, we now determine the relaxation rate of our probe qubit due to in-sample polarization fluctuations. To do so, we compute magnetic noise at the location of the probe qubit due to these fluctuations. In particular, by Eq. S7 and S8, we need to compute:

$$\langle [B_-(\mathbf{r}, t), B_+(\mathbf{r}, 0)] \rangle = \frac{\mu_0^2}{L^2} \sum_{\mathbf{q}_1, \mathbf{q}_2} \int \frac{d\omega_1 d\omega_2 dz'_1 dz'_2}{(2\pi)^2} H_i^-(z'_1, \mathbf{q}_1, \omega_1) H_j^+(z'_2, \mathbf{q}_2, \omega_2) \quad (\text{S73})$$

$$\times \langle [P_i(z'_1, \mathbf{q}_1, \omega_1), P_j(z'_2, \mathbf{q}_2, \omega_2)] \rangle e^{i(\mathbf{q}_1 \cdot \mathbf{r} - \omega_1 t)} e^{-i\omega_2 t} \quad (\text{S74})$$

where  $\mathbf{r} = (\rho, d) = (0, 0, d)$  is the location of the qubit. Assuming space-time translation invariance, we have that

$$\langle [P_i(z'_1, \mathbf{q}_1, \omega_1), P_j(z'_2, \mathbf{q}_2, \omega_2)] \rangle = 2\pi\delta(\omega_1 + \omega_2)\delta_{\mathbf{q}_1, -\mathbf{q}_2} \langle [P_i(z'_1, \mathbf{q}, \omega), P_j(z'_2, -\mathbf{q}, -\omega)] \rangle \quad (\text{S75})$$

Thus, the magnetic noise can be expressed as:

$$\langle [B_-(\mathbf{r}, t), B_+(\mathbf{r}, 0)] \rangle = \frac{\mu_0^2}{L^2} \sum_{\mathbf{q}} \int \frac{d\omega dz'_1 dz'_2}{(2\pi)^2} H_i^-(z'_1, \mathbf{q}, \omega) H_j^-(z'_2, -\mathbf{q}, -\omega) \langle [P_i(z'_1, \mathbf{q}, \omega), P_j(z'_2, -\mathbf{q}, -\omega)] \rangle e^{-i\omega t} \quad (\text{S76})$$

To proceed further, we simply need to contract the product of kernels with the polarization commutator:

$$H_i^-(1) H_j^+(2) \langle [P_i(1), P_j(1)] \rangle = \left\langle \left[ \frac{1}{2} (H_+^-(1) P_-(1) + H_-^-(1) P_+(1)) + H_z^-(1) P_z(1), \right. \right. \quad (\text{S77})$$

$$\left. \frac{1}{2} (H_+^+(2) P_-(2) + H_-^+(2) P_+(2)) + H_z^+(2) P_z(2) \right] \rangle \quad (\text{S78})$$

$$= \frac{1}{4} (H_+^-(1) H_+^+(2) \langle [P_-(1), P_+(2)] \rangle + H_-^-(1) H_+^+(2) \langle [P_+(1), P_-(2)] \rangle + H_z^-(1) H_z^+(2) \langle [P_z(1), P_z(2)] \rangle) \quad (\text{S79})$$

$$+ \frac{1}{4} (H_+^-(1) H_+^+(2) \langle [P_-(1), P_-(2)] \rangle + H_-^-(1) H_+^+(2) \langle [P_+(1), P_+(2)] \rangle) \quad (\text{S80})$$

$$+ \frac{1}{2} (H_+^-(1) H_z^+(2) \langle [P_-(1), P_z(2)] \rangle + H_-^-(1) H_z^+(2) \langle [P_+(1), P_z(2)] \rangle) \quad (\text{S81})$$

$$+ H_z^-(1) H_+^+(2) \langle [P_z(1), P_+(2)] \rangle + H_z^-(1) H_+^+(2) \langle [P_z(1), P_-(2)] \rangle) \quad (\text{S82})$$

where  $H_i^-(1) = H_i^-(d, z_1, \mathbf{q}_1, \omega)$ ,  $H_j^+(2) = H_j^+(d, z_2, \mathbf{q}_2, \omega')$ ,  $P_i(1) = P_i(z_1, \mathbf{q}_1, \omega)$ , and  $P_j(2) = P_j(z_2, \mathbf{q}_2, \omega')$ . The first line is the only line that appreciably contributes if we assume that our sample is rotationally invariant or has a conserved polarization density. Now we compute the product of the kernels in the approximation that  $\omega/c \ll q$ . We remark that:

$$H_i^+ = H_i^x + iH_i^y = [(-q_y\delta_{iz} + i\lambda\delta_{iy}) + (\lambda\delta_{ix} + iq_x\delta_{iz})] \frac{\omega}{2\lambda} e^{-\lambda|z-z'|} = [iq_+\delta_{iz} + 2\lambda\delta_{i-}] \frac{\omega}{2\lambda} e^{-\lambda|z-z'|} \quad (\text{S83})$$

$$H_i^- = H_i^x - iH_i^y = [(-q_y\delta_{iz} + i\lambda\delta_{iy}) + (-\lambda\delta_{ix} - iq_x\delta_{iz})] \frac{\omega}{2\lambda} e^{-\lambda|z-z'|} = -[iq_-\delta_{iz} + 2\lambda\delta_{i+}] \frac{\omega}{2\lambda} e^{-\lambda|z-z'|} \quad (\text{S84})$$

Now, just to get an estimate for the magnetic field strength, we compute only two of these kernels and use Gaussian polarization correlations to get an estimate for the noise signal. In particular, we compute

$$H_+^-(1) H_-^+(2) = \frac{\omega^2}{4\lambda^2} e^{-\lambda|z-z'_1|} e^{-\lambda|z-z'_2|} 4\lambda^2 \approx \omega^2 e^{-q|z-z'_1|} e^{-q|z-z'_2|} \quad (\text{S85})$$

$$H_z^-(1) H_z^+(2) = \frac{\omega^2}{4\lambda^2} e^{-\lambda|z-z'_1|} e^{-\lambda|z-z'_2|} q^2 \approx \frac{\omega^2}{4} e^{-q|z-z'_1|} e^{-q|z-z'_2|} \quad (\text{S86})$$

which would be the only non-zero terms if the system was translation and rotationally invariant.

Thus, we have that the total noise expression looks something like:

$$\frac{1}{T_1} = \frac{\mu_z^2}{4} \coth\left(\frac{\beta\omega}{2}\right) \int_{-\infty}^{\infty} dt \langle [B^-(\mathbf{r}, t), B^+(\mathbf{r}, 0)] \rangle e^{i\omega t} \quad (\text{S87})$$

$$= \frac{\mu_z^2 \mu_0^2 \omega^2}{4} \coth\left(\frac{\beta\omega}{2}\right) \int \frac{d^2\mathbf{q}}{(2\pi)^2} \int dz'_1 \int dz'_2 \frac{e^{-q|z-z'_1|} e^{-q|z-z'_2|}}{4} [C_{+-} + C_{zz}] \quad (\text{S88})$$

where  $\mathcal{C}_{+-} = \langle [P_+(1), P_-(2)] \rangle$  and  $\mathcal{C}_{zz} = \langle [P_z(1), P_z(2)] \rangle$ . Now, assuming that we have a 2D sample, our polarization only fluctuates in-plane (hence we can neglect  $\mathcal{C}_{zz}$ ), and Gaussian correlations, we can compute the retarded correlations (see next section for a derivation of this):

$$\chi_{+-} = \frac{Q^2 \hbar}{a^4} \frac{1}{\rho \omega_d^2 - (\omega + i\eta)^2} \delta(d - z'_1) \delta(d - z'_2) \quad (\text{S89})$$

where  $\omega_d = \sqrt{c_s^2 q^2 + \omega_0^2}$  and  $\mathcal{C}_{+-} = \text{Im}[\chi_{+-}]$ . We can plug this in to get an estimate for the magnetic noise as:

$$\frac{1}{T_1} = \frac{\mu_z^2 \mu_0^2 \omega^2}{16} \coth\left(\frac{\beta \omega}{2}\right) \left(\frac{Q^2 \hbar}{a^{2d} \rho}\right) \times \begin{cases} \left[e^{-2q_{\text{res}} d} \frac{\pi}{2c_s^2}\right] & \omega_0 \leq \omega \\ 0 & \omega_0 > \omega \end{cases} \quad (\text{S90})$$

If we divide this by the estimate for the electrical noise in the main text, we find that the ratio between these two is controlled by the dimensionless ratio:

$$\frac{(1/T_1)_{\text{magnetic}}}{(1/T_1)_{\text{electric}}} \sim \frac{\mu_z^2 \omega^2}{d_{\perp}^2 q_{\text{res}}^2 c^4} = \frac{\mu_z^2 c_s^2}{d_{\perp}^2 c^4} \sim 10^{-4} \quad (\text{S91})$$

for the parameters shown in the main text.

### DERIVATION OF NUMERICAL ESTIMATE OF $1/T_1$

In the main text, we made a numerical prediction for the magnitude of  $1/T_1$  as a function of frequency ( $\omega$ ), qubit-sample distance ( $d$ ), and temperature ( $T$ ) for a qubit above a dielectric material with non-interacting phonon modes. For transparency, we provide on the precise derivation of the dimensionful prefactor to Eq. 4 of the main text. Namely, consider once again the toy-model of a ionic crystal considered in the main text (see Fig 2(a,b) of the main text). We can associate with each sublattice a phonon displacement field ( $\mathbf{u}_+$  and  $\mathbf{u}_-$  for the positive and negative ions respectively). For the lattice, there will be two classes of phonon modes: gapless acoustic branches  $\mathbf{u}_{ac} = (\mathbf{u}_+ + \mathbf{u}_-)/2$  and gapped optical branches  $\mathbf{u} = (\mathbf{u}_+ - \mathbf{u}_-)$ . Since acoustic phonons don't carry polarization, we characterize the dynamics of the optical phonons by the (Euclidean) action [2]:

$$S_u = \int_0^{\hbar\beta} d\tau \int d^d x \frac{\rho}{2} u_j(x) [(-\partial_0^2 + \omega_T^2) \delta_{jl} - c_T^2 (\nabla^2 \delta_{jl} - \partial_j \partial_l) - c_L^2 \partial_j \partial_l] u_l(x) \quad (\text{S92})$$

where  $\beta$  is the inverse temperature,  $\rho$  is the mass density of the lattice,  $c_{T,L}$  refer to the transverse and longitudinal phonon velocity, and  $\omega_T$  indicates the phonon mass. For sake of analytic tractability, we have neglected interactions between phonon modes. These phonon modes are related to the polarization via:

$$\mathbf{P} = \frac{Q}{a^d} \mathbf{u} \quad (\text{S93})$$

where  $Q$  is the Born effective charge of the material. Since these phonon modes generate a polarization, we must also account for the coupling between the phonon modes and the electromagnetic field. Since the electromagnetic potential will only couple to the longitudinal optical phonon mode, this is characterized by the action:

$$S_\varphi = \int_0^{\hbar\beta} d\tau \int d^d r \left[ \frac{\varepsilon}{8\pi} (\nabla \varphi)^2 + iQ\varphi \partial_j u_j \right] \quad (\text{S94})$$

where  $\varphi$  is the electromagnetic potential,  $Q$  is the charge of the crystal's ions, and  $\varepsilon$  is the dielectric constant of the material. Integrating out these electromagnetic field degrees of freedom generates a phonon-phonon interaction of the form:

$$S'_u = \frac{2\pi Q^2}{\varepsilon\beta} \sum_{n,\mathbf{q}} \frac{q_i^2 u_i^\dagger(\omega_n, \mathbf{q}) u_i(\omega_n, \mathbf{q})}{q^2} \quad (\text{S95})$$

where the sum over  $n$  is a sum over Matsubara frequencies  $\omega_n = \frac{2\pi n}{\beta}$  where  $n \in \mathbb{Z}$  and  $\mathbf{u}(\omega_n, \mathbf{q})$  is related  $\mathbf{u}(\tau, x)$ :

$$u_j(\tau, x) = \frac{1}{\sqrt{\hbar\beta}} \sum_n e^{i\omega_n \tau} \frac{1}{L^{d/2}} \sum_{\mathbf{q}} e^{i\mathbf{q} \cdot \mathbf{x}} u_j(\omega_n, \mathbf{q}). \quad (\text{S96})$$

Note that the action of Eq. S95 effectively renormalizes the mass of the longitudinal optical phonon mode to  $\sqrt{\left(\frac{4\pi Q^2}{\epsilon}\right) + \omega_T^2}$  and as such this mode will have a gap even if  $\omega_T$  is small (which will be our assumption). Hence, we can integrate out these modes to capture the low-energy dynamics. As such, our effective action, written using the Matsubara modes of Eq S96, is given by:

$$S_{\text{eff}} = \sum_{n, \mathbf{q}} \frac{\rho}{2} u_j^\dagger [(\omega_n^2 + \omega_T^2) \delta_{jl} + c_T^2 q^2] \frac{q^2 \delta_{jl} - q_j q_l}{q^2} u_l. \quad (\text{S97})$$

Now, if we impose  $\partial_j u_j = 0$ , the integrand of our effective action is invertible and one can easily extract the two-point polarization correlations  $\langle P_+^\dagger(\omega_n, \mathbf{q}) P_-(\omega_m, \mathbf{q}) \rangle = \frac{Q^2}{a^{2d}} \langle u_+^\dagger(\omega_n, \mathbf{q}) u_-(\omega_n, \mathbf{q}) \rangle = \chi_{+-}(\omega_n, \mathbf{q})$ :

$$\chi_{+-}(\omega_n, \mathbf{q}) = \frac{Q^2 \hbar}{a^{2d} \rho} \frac{1}{\omega_d^2 + \omega_n^2} \quad (\text{S98})$$

where  $\omega_d = \sqrt{c_T^2 q^2 + \omega_T^2}$ . Note that this can be transformed into the retarded correlation function by rotating  $i\omega_n \rightarrow \omega + i\eta$  yielding:

$$\chi_{+-}(\omega, \mathbf{q}) = \frac{Q^2 \hbar}{a^{2d} \rho} \frac{1}{\omega_d^2 - (\omega + i\eta)^2} \quad (\text{S99})$$

Since, it is the imaginary component of  $\chi_{+-}$  that enters into the expression for  $T_1$  (Eq. S62), we note that:

$$\text{Im} \left[ \frac{1}{\omega_d^2 - (\omega + i\eta)^2} \right] = \frac{\pi}{2\omega_d} [\delta(\omega_d - \omega) - \delta(\omega_d + \omega)] \quad (\text{S100})$$

where we took  $\eta \rightarrow 0$  in the last step. Thus, since  $\delta(\omega_d - \omega) = \frac{\sqrt{c_T^2 q_{res}^2 + \omega_T^2}}{c_T^2 q_{res}} \delta(q - q_{res}) = \frac{\omega}{c_T^2 q_{res}} \delta(q - q_{res})$ , where  $q_{res} = \frac{\sqrt{\omega^2 - \omega_T^2}}{c_T}$ , we have that

$$\frac{1}{T_1} = \frac{1}{4} \mu_0^2 d_\perp^2 \coth \left( \frac{\beta \hbar \omega}{2} \right) \left[ \frac{c^4}{16\pi} \frac{Q^2 \hbar}{\rho a^4} \right] \times \begin{cases} \left[ e^{-2q_{res} d} \frac{\pi}{2c_T^2} q_{res}^2 \right] & \omega_T \leq \omega \\ 0 & \omega_T > \omega \end{cases} \quad (\text{S101})$$

from which we get the numerical prediction of  $1/T_1$ . Note that in this section, we referred to the transverse optical phonon mode mass and velocity as  $\omega_T$  and  $c_T$  respectively (to distinguish it from the longitudinal optical phonon mode). To make contact with the notation of the main text, simply relabel  $\omega_T \rightarrow \omega_0$  and  $c_T \rightarrow c_s$ .

## DERIVATION OF $1/T_1$ SCALING ACROSS PARA-TO-FERROELECTRIC PHASE TRANSITIONS

In this section, we provide additional details regarding how qubit sensors can shed light on paraelectric-to-ferroelectric phase transitions. We start with an intuitive real space argument for distance scaling of noise, which hints towards a possible enhancement of  $1/T_1$  as we approach the critical point. We next consider a thermal (classical) phase transition where we detail the precise derivation and additional intuition of the scaling theory of the main text. We conclude by doing the same for the quantum case.

### Intuitive Real Space Argument for Distance Scaling of $1/T_1$

In the main text, we claimed that studying the qubit-sample distance scaling of  $1/T_1$  can provide a tell-tale signature of approaching the critical point. To justify this, we provide some intuition for the distance scaling of the noise away from and near the critical regime, based on a simple real-space picture. Roughly speaking, the relaxation rate of the qubit can be expressed as the frequency-filtered correlation function of electric fields generated by polarization fluctuations. Since the qubit is sensitive to polarization fluctuations on an area of size  $d^2$  within the 2d sample (corresponding to the solid angle subtained by the qubit at the sample), the relaxation rate takes the following form:

$$\frac{1}{T_1} \sim \sum_{i,j} \langle E_i E_j \rangle_\omega \sim \sum_{i,j} \left\langle \frac{P_i}{d^3} \frac{P_j}{d^3} \right\rangle_\omega \sim \frac{1}{d^6} \times d^2 \times \sum_i \langle P_i P_0 \rangle_\omega = \frac{1}{d^4} \langle P_i P_0 \rangle_\omega \quad (\text{S102})$$



where we used translation invariance of the correlation function in the third step to integrate over the ‘center of mass’ coordinate which gives an extra factor of  $d^2$ . For low frequencies, we may expect that the polarization correlator  $\langle P_i P_0 \rangle_\omega$  is not very different from the static correlator  $\langle P_i P_0 \rangle_{\omega \rightarrow 0}$  (we will revise this crude approximation later within specific models). Therefore, if the sample-probe distance  $d$  is larger than the correlation length  $\xi$ , the correlator yields  $\xi^2$ . This happens when we are far enough from the critical point so that  $\xi$  is small, or when the sample is quite far so that  $d$  is large. In this regime,  $1/T_1$  scales as  $d^{-4}$ . In contrast, when we are close to the sample or near the critical point so that  $d \ll \xi$ , then the correlator yields  $d^2$ . So, naively we expect  $1/T_1$  to scale as  $d^{-2}$ , although the precise scaling will depend on the nature of the dynamics near the critical point. Therefore, a change in the scaling of  $1/T_1$  as a function of distance can signal criticality, as argued in the main text.

### Derivation of $1/T_1$ near thermal ferroelectric transition: Mean-field theory and scaling theory

As discussed in the main text, the transition between a paraelectric and a ferroelectric occurs due to the softening of the transverse optical phonon mode. Specifically, the gap  $\omega_0$  of this mode decreases as one lowers the temperature, and  $\omega_0 \xrightarrow{T \rightarrow T_c} 0$ . Near the critical regime, the temperature  $T \sim T_c$  is much larger than the gap and so there is always a large occupancy of this mode and accordingly the considerations of classical hydrodynamics of a critical mode will apply. The dynamics of the polarization in the critical regime (and consequently the scaling theory of dynamical correlations) are strongly constrained by conservation laws. In our case of interest, the order parameter (polarization density) is an Ising order parameter, which is not conserved by the dynamics. We further assume that we can neglect coupling of the order parameter to a diffusive mode (such as conserved energy density). Thus, following Refs. [3–5], we can write down the expression for the dynamic electrical susceptibility at a mean-field level.

$$\chi(\mathbf{q}, \omega) \propto \frac{1}{-i\omega/\Gamma + \mathbf{q}^2 + \xi^{-2}} \quad (\text{S103})$$

where  $\xi^{-1} \propto |T - T_c|$  is the inverse correlation length, and  $\Gamma$  determines the rate of approach to thermal equilibrium after a perturbation. Using this expression for  $\chi(\mathbf{q}, \omega)$ , we evaluate the mean-field scaling of  $1/T_1$  as a function of distance. Specifically, we find that in the experimentally relevant limit of small qubit splitting ( $\omega \rightarrow 0$ ):

$$\frac{1}{T_1} \sim \frac{2T}{\omega} \int_0^\infty dq q^3 e^{-2qd} \text{Im}[\chi(q, \omega)] \xrightarrow{\omega \rightarrow 0} \begin{cases} \frac{T}{\Gamma} \ln\left(\frac{\omega d^2}{\Gamma}\right), & d \ll \xi \\ \frac{T\xi^4}{\Gamma d^4}, & d \gg \xi \end{cases} \quad (\text{S104})$$

As argued in the previous subsection, we recover the  $d^{-4}$  behavior of  $1/T_1$  away from criticality ( $d \gg \xi$ ), where mean-field theory is expected to be reasonably accurate. However, it may break down in 2D near criticality, and therefore we resort to a more general scaling theory for  $1/T_1$ . Near the critical point, the behavior is characterized by the following scaling form of the dynamic electrical susceptibility (assuming spatial isotropy for):

$$\chi(\mathbf{q}, \omega) = \chi(\mathbf{q}) Y(\omega q^{-z}, q\xi), \text{ where } \chi(q) \equiv \chi(q, 0) \sim q^{-2+\eta} \text{ and } Y(0, q\xi) = 1 \quad \forall q \quad (\text{S105})$$

At the critical point,  $\xi \rightarrow \infty$  and therefore,  $\chi(\mathbf{q}, \omega) \sim q^{-2+\eta} Z(\omega q^{-z})$ , using this gives the following scaling form for  $1/T_1$ :

$$\frac{1}{T_1} \sim \frac{2T}{\omega} \int_0^\infty dq q^3 e^{-2qd} \times q^{-2+\eta} Z(\omega q^{-z}) = \frac{2T}{\omega d^{2+\eta}} \Phi(\omega d^z) \quad (\text{S106})$$

Note that the above form implies that there is an apparent divergence in  $1/T_1$  as  $\omega \rightarrow 0$ . However, this is somewhat misleading, as general considerations imply that  $\text{Im}[\chi(\mathbf{q}, \omega)]$  is necessarily odd in  $\omega$  [6]. Therefore, we can recast this scaling form by defining  $\Phi(\omega d^z) = \omega d^z \Psi(\omega d^z)$ :

$$\frac{1}{T_1} \sim \frac{2T}{d^{2+\eta-z}} \Psi(\omega d^z) \quad (\text{S107})$$

which was the result quoted in Eq. (4) in the main text. The mean-field  $d$ -scaling of  $1/T_1 \sim \ln(\omega d^2)$  discussed earlier may be found from the more general scaling expression in Eq. (S107) by using mean-field critical exponents  $\eta = 0$  and  $z = 2$  [5], and using the scaling function  $\Psi(x) = \ln(x)$ .

### Derivation of $1/T_1$ near quantum ferroelectric transition

We now turn our attention to the quantum para-to-ferroelectric phase transition, and derive the appropriate scaling relations for  $1/T_1$ . Unlike the classical case where one needs to supplement the free-energy by additional phenomenological equations of motion of the order parameter, the quantum dynamics of polarization is completely determined by the Hamiltonian [6]. Furthermore, energy is always conserved if the Hamiltonian is time-independent. Therefore, in principle, once we know the quantum Hamiltonian we should be able to extract all dynamical correlations. In practice this often turns out to be quite difficult, and therefore one has to resort to certain limiting cases.

We consider the experimentally relevant limit of very low frequencies ( $\omega \ll T$ ). In this regime, the quantum dynamics is typically relaxational and its description using weakly interacting soft modes is not accurate [6]. Nevertheless, we can write down a generic scaling function analogous to the classical case, which includes an additional scaling variable  $\omega_0/T$ , where  $\omega_0$  is the gap of the soft mode that closes at  $T = 0$  and  $\lambda = \lambda_c$ , the quantum critical point.

$$\chi(\mathbf{q}, \omega) = \chi(\mathbf{q}) Y_q \left( \frac{\omega}{T}, \frac{\omega_0}{T}, \frac{c_s q}{T} \right), \text{ where } \chi(q) \sim q^{-2+\eta} \text{ as in the classical case} \quad (\text{S108})$$

where  $Y_q$  is a dimensionless quantum scaling function. Plugging this into Eq. (3) in the main text gives the relaxation rate as:

$$\frac{1}{T_1} \sim \frac{2T}{\omega} \int_0^\infty dq q^3 e^{-2qd} \text{Im}[\chi(\mathbf{q}, \omega)] = \frac{1}{d^{2+\eta}} \Psi \left( \frac{\omega}{T}, \frac{\omega_0}{T}, \frac{c_s}{Td} \right) \quad (\text{S109})$$

While the scaling relation in Eq. (S109) is formally correct, it unfortunately does not give us a lot of information. Therefore, it is useful to resort to a more phenomenological form of  $\chi(\mathbf{q}, \omega)$  which cannot be rigorously derived analytically, but is nevertheless well-motivated and more predictive for the behavior of  $1/T_1$  in the small  $\omega/T$  limit (the dynamical critical exponent  $z = 1$  for this transition, but we keep a general  $z$ ).

$$\chi(\mathbf{q}, \omega) = \frac{\chi(0, 0)}{1 - i\omega/\Gamma + q^2 \xi^2}, \text{ where } \Gamma \sim T, \quad \xi \sim \frac{c_s}{T^{1/z}} \text{ and } \chi(0, 0) \sim T^{(-2+\eta)/z} \quad (\text{S110})$$

To motivate the form of  $\chi(\mathbf{q}, \omega)$  in the vicinity of the quantum critical point, we make the following observations. First, we expect a finite relaxation rate  $\Gamma$  towards equilibrium even at  $q = 0$  (as the order parameter is not-conserved), and finite  $q$  corrections are expected to be analytic at non-zero  $T$  when  $\lambda \approx \lambda_c$ . Second, we note that exactly at the critical value of the tuning parameter, i.e.,  $\lambda = \lambda_c$ , the static uniform susceptibility  $\lim_{q \rightarrow 0} \chi(q, 0)$  only diverges at  $T = 0$ , but remains finite at non-zero  $T$  with a correlation length  $\xi$ . Next, since the only energy-scale in the quantum critical regime is  $T$ , we must have  $\Gamma \sim T$ , and  $\xi \sim c_s/T^{1/z}$  (which corresponds to a smaller correlation length at larger  $T$  due to thermal fluctuations). Finally, static scaling theory requires that  $\chi(q, 0) \sim q^{-2+\eta}$  at  $T = 0$  and obeys a scaling relation of the form  $\chi(q, 0) = q^{-2+\eta} X(q\xi)$  for any  $T$ . Non-divergence of  $\chi(q, 0)$  at finite  $T > 0$  then essentially fixes  $\chi(0, 0) \sim T^{(-2+\eta)/z}$ . Thus, we have all the ingredients to arrive at the postulated form of  $\chi(\mathbf{q}, \omega)$  in Eq. (S110). We note that a similar form is an excellent approximation to the low-frequency dynamics of the one-dimensional by comparing with the exact solution [6, 7]; our arguments show that this should be true for non-conserved dynamics in 2D as well. Using Eq. (S110), we can derive the scaling of  $1/T_1$  for small  $\omega/T$ :

$$\frac{1}{T_1} \sim \frac{2T}{\omega} \int_0^\infty dq q^3 e^{-2qd} \text{Im}[\chi(\mathbf{q}, \omega)] = \frac{2T\chi(0, 0)}{\Gamma T} \int dq \frac{q^3 e^{-2qd}}{(1 + q^2 \xi^2)^2} \propto \begin{cases} T^{(2+\eta)/z} \ln \left( \frac{c_s}{dT^{1/z}} \right), & d \ll \xi_T \\ T^{(-2+\eta)/z} d^{-4}, & d \gg \xi_T \end{cases} \quad (\text{S111})$$

which is Eq. (6) in the main text. We note that just like the classical case, the distance-scaling of  $1/T_1$  is  $d^{-4}$  for  $d$  much larger than the correlation length  $\xi$  (i.e., away from criticality), but is significantly altered as we approach the critical point ( $\lambda = \lambda_c$  and  $T = 0$ ).

### DERIVATION OF DISPERSION RELATION FOR DIPOLARON MODE

In this section, we derive the dipolaron dispersion for a two-dimensional fluid of electrically neutral dipolar molecules. Like plasmons in a charged Fermi liquid, dipolarons are longitudinal collective modes that arise due to long-range electrostatic interactions in dipolar fluids. We know that nature of plasmons in a Fermi liquid differ drastically between two and three spatial dimensions — in  $d = 3$ , plasmons are gapped excitations at  $\mathbf{q} = 0$ , while in  $d = 2$ , they are gapless with a dispersion  $\omega_p(\mathbf{q}) \propto \sqrt{q}$ . The reason is the weaker electric field created by two dimensional charge imbalance results in a weaker restoring force at large distances, compared to a three dimensional charge imbalance.

Such an effect is at play for dipolarons too, resulting in gapless dispersion  $\omega_d^2(\mathbf{q}) \sim aq^2 + bq^3$  for dipolarons in two dimensions. In what follows, we derive this dispersion from a simple hydrodynamic treatment of dipolar density fluctuations. We note that our results are in accordance with more a microscopic treatment of collective modes in two-dimensional dipolar gases [8].

Consider a fluid of dipolar molecules at equilibrium density  $n_d$  at chemical potential  $\mu_{eq}$  and equilibrium velocity  $\mathbf{v}_0 = 0$ . Now we consider fluctuations about the mean density so that there is local density profile  $\delta n(\mathbf{r}, t) = n(\mathbf{r}, t) - n_d$ , and velocity  $\mathbf{v}(\mathbf{r}, t) \neq 0$ . The linearized continuity and Euler's (force) equation read:

$$\partial_t \delta n(\mathbf{r}, t) + n_d \nabla \cdot \mathbf{v} = 0, \quad mn_d \partial_t \mathbf{v} = -n_d \nabla \left( \mu_{eq} + \frac{\partial \mu}{\partial n} \delta n \right) - \nabla (\boldsymbol{\mu} n_d \cdot \mathbf{E}) \quad (\text{S112})$$

The generated electric field can be related to the fluctuating polarization density  $\boldsymbol{\mu} n(\mathbf{r})$  as discussed previously (neglecting retardation effects):

$$E_i(\mathbf{r}, t) = \int d\mathbf{r}' T_{ij}^d(\mathbf{r}, \mathbf{r}') \mu_j n(\mathbf{r}', t), \quad T_{ij}^d(\mathbf{q}) = \int d^d r e^{i\mathbf{q} \cdot \mathbf{r}} \partial_i \partial_j \left( \frac{1}{r} \right) = \begin{cases} -\frac{4\pi q_i q_j}{q^2}, & D = 3 \\ -\frac{2\pi q_i q_j}{q}, & D = 2 \end{cases} \quad (\text{S113})$$

Going to momentum space and using that the compressibility is given by  $\kappa = n_d^2 (\frac{\partial \mu}{\partial n})$ , we can combine Eqs. (S112) to find the following equation for  $\delta n(\mathbf{q}, \omega)$ :

$$\omega^2 \delta n(\mathbf{q}, \omega) = \left( \frac{\kappa}{mn_d} \mathbf{q}^2 + \frac{\mu_i \mu_j n_d}{m} q_i T_{ij}^d(\mathbf{q}) q_j \right) \delta n(\mathbf{q}, \omega) \quad (\text{S114})$$

Using the form of  $T_d$  from Eq. (S113) for  $D = 2$ , we finally get the collective mode dispersion in  $D = 2$  that was quoted in the main text:

$$\omega_d^2(\mathbf{q}) = v^2 q^2 + \frac{2\pi n_d q(\mathbf{q} \cdot \boldsymbol{\mu})^2}{m} \quad (\text{S115})$$

where  $v = \sqrt{\kappa/mn_d}$  is the speed of the collective mode at small  $\mathbf{q}$ . This is analogous to the linearly dispersing zero sound mode in Fermi liquids, and does not require dipolar interactions. At larger dispersion, anisotropy effects due to dipolar interactions come into play and we have a dominating  $q^{3/2}$  term in the dispersion. In particular, if we take the angular average over all directions of  $\boldsymbol{\mu}$  (which can point anywhere on the 2-sphere), then we can replace  $(\mathbf{q} \cdot \boldsymbol{\mu})^2 \rightarrow q^2 \mu^2/3$ , and we recover the dispersion in Ref. 8.

$$\omega_d^2(\mathbf{q}) = c_s^2 q^2 + \frac{2\pi \mu^2 n_d q^3}{3m} \quad (\text{S116})$$

## DERIVATION OF POLARIZATION CORRELATIONS FOR RELAXOR FERROELECTRIC MODEL

In the main text, we investigated the relaxation rate of a qubit sensor in the vicinity of a relaxor ferroelectric modeled via the Hamiltonian:

$$H = \sum_i \left[ \frac{\Pi_i^2}{2M} + V(u_i) \right] - \frac{1}{2} \sum_{i,j} v_{ij} u_i u_j - \sum_i E_i^{\text{ext}} u_i - \sum_i h_i u_i \quad (\text{S117})$$

where  $\Pi_i = M\dot{u}_i$  is the conjugate momentum of the polarization-carrying displacement  $u_i$  (chosen to be in the  $z$ -direction),  $M$  is the effective mass,  $E_i^{\text{ext}}$  is an external applied field,  $h_i \sim N(0, \Delta)$  is a random field,  $V(u_i) = \frac{\kappa}{2} u_i^2 + \frac{\gamma}{4} u_i^4$  ( $\kappa, \gamma > 0$ ), and

$$v_{ij} = -\frac{1}{|\mathbf{r}_i - \mathbf{r}_j|^3} \quad \text{if } i \neq j \quad (\text{S118})$$

is the dipolar interaction and  $\mathbf{r}_i = (x_i, y_i, 0)$  is the 2D lattice coordinate of the  $i^{\text{th}}$  dipole. In this section, we provide details for how we derived the form of the qubits relaxation rate. We do so by computing the disorder-averaged polarization fluctuations arising from the above Hamiltonian, following the derivation in Refs. [9–11]. In general, this is hard to do because of (i) the anisotropic and long-range nature of the dipolar interaction and (ii) the anharmonicity of the local potential. We treat the former by using the leading order correction to mean field (the Onsager approximation) because such fluctuations are important in the relaxor context and we treat the latter using

a quasi-harmonic approximation (we linearize the equations of motion). With this in mind, we write the equations of motion under Eq. S117 as:

$$M\ddot{u}_i = -\frac{dV(u_i)}{du_i} - h_i u_i - E_i^{\text{local}} \quad \text{where} \quad E_i^{\text{local}} = \sum_j v_{ij} u_j + E_i^{\text{ext}} \quad (\text{S119})$$

To simplify this Hamiltonian, we can make a mean-field approximation:

$$E_i^{\text{local}} \approx E_i^{\text{MF}} = \sum_j v_{ij} \langle u_j \rangle + E_i^{\text{ext}} - \lambda \langle u_i \rangle \quad (\text{S120})$$

where  $\langle \dots \rangle$  indicates thermal averaging and we introduced the Lagrange multiplier  $-\lambda \langle u_i \rangle$  which is used to enforce the fluctuation-dissipation theorem for the polarization fluctuations we compute [12]. It is precisely this Lagrange multiplier that enables incorporating fluctuations, to leading order. This yields:

$$H \approx \sum_i H_i = \sum_i [H_i^0 - h_i u_i - E_i^{\text{MF}} u_i] \quad (\text{S121})$$

where  $H_i^0 = \frac{\Pi_i^2}{2M} + V(u_i) - (\lambda/2)u_i^2$ .

### Self-Consistent Equations for Phonon Dispersion

Given the model derived above, we can compute the phonon dispersion self-consistently which will consequently determine the form of the dipolar fluctuations that enter our expression for  $1/T_1$ . To do so, we aim to compute the dielectric susceptibility  $\chi(\omega, \mathbf{q}) = \overline{\delta \langle u(\omega, \mathbf{q}) \rangle} / \delta E^{\text{ext}}(\omega, \mathbf{q})$  where  $\delta \langle u(\omega, \mathbf{q}) \rangle$  indicates deviation of the displacement field from its thermal expectation and  $\overline{\dots}$  indicates averaging over disorder realizations. We do this by defining an auxiliary susceptibility,  $\varphi_{h_i}(\omega)$ , which characterizes the system's susceptibility to the local mean field:

$$\delta \langle u_i(\omega) \rangle = \varphi_{h_i}(\omega) E_i^{\text{MF}}(\omega). \quad (\text{S122})$$

Now we disorder average both sides of this expression and take the 2D discrete Fourier transform of both sides. In doing so, we assume that the effects of the random fields decouple in  $\varphi_{h_i}(\omega)$  and  $\langle u_i \rangle$  implying that  $\overline{\varphi_{h_i}(\omega)} = \overline{\varphi_h}(\omega)$  which only has a  $\mathbf{q} = 0$  component. This yields:

$$\overline{\delta \langle u(\omega, \mathbf{q}) \rangle} = \overline{\varphi_h}(\omega) \left[ v_{\mathbf{q}} \overline{\delta \langle u(\omega, \mathbf{q}) \rangle} - \lambda \overline{\delta \langle u(\omega, \mathbf{q}) \rangle} + \delta E^{\text{ext}}(\omega, \mathbf{q}) \right]. \quad (\text{S123})$$

Note that, in the above expression,  $v_{\mathbf{q}}$  is the 2D discrete Fourier transform of the dipolar interaction with the assumption that the dipoles are arranged in a square lattice. The precise form of this discrete Fourier transform was worked out in Refs. [13, 14] and was found to be:

$$v_{\mathbf{q}}/n = \frac{1}{n} \sum_{i,j} v_{i,j} e^{i\mathbf{q} \cdot (\mathbf{r}_i - \mathbf{r}_j)} \approx v_0 \left( 1 - \frac{3}{4\pi f} |\mathbf{q}| \right) \quad \text{with} \quad v_0 = \frac{8\pi}{3} f \quad (\text{S124})$$

where  $f$  is a lattice specific constant and is  $f = 1.078$  for a simple cubic lattice. Using Eq. S123, we see that the dielectric susceptibility can be written as:

$$\chi(\omega, \mathbf{q}) = \frac{\overline{\delta \langle u(\omega, \mathbf{q}) \rangle}}{\delta E^{\text{ext}}(\omega, \mathbf{q})} = \frac{1}{\overline{\varphi_h}(\omega)^{-1} - (v_{\mathbf{q}} - \lambda)}. \quad (\text{S125})$$

Expression in hand, we can now use the classical equations of motion of the displacement field under the Hamiltonian of Eq. S121 to directly compute the form of  $\overline{\varphi_h}(\omega)$  from which the above susceptibility can be computed directly. The equations of motion are:

$$M\ddot{u}_i = -\frac{dV(u_i)}{du_i} + \lambda u_i + h_i + E_i^{\text{MF}} - \Gamma \dot{u}_i = -(\kappa - \lambda)u_i - \gamma u_i^3 + h_i + E_i^{\text{MF}}(t) - \Gamma \dot{u}_i \quad (\text{S126})$$

where we introduced a phenomenological decay  $\Gamma$  to regulate our response functions. At the end, we will take  $\Gamma \rightarrow 0$ . Now, to treat this equation analytically, we linearize it by treating deviations of the displacement from its disorder



and thermal average to be small  $u_i(t) = p + \delta u_i(t)$  where  $p = \overline{\langle u_i(0) \rangle}$  is the static mean displacement field. Note that, here,  $\delta u_i(t)$  contains all of the time dependence of  $u_i(t)$  and is not in general zero after thermal and disorder averaging. This yields:

$$M\delta\ddot{u}_i(t) = -(\kappa - \lambda)(p + \delta u_i) - \gamma(p^3 + 3p^2\delta u_i + 3p\delta u_i^2 + \delta u_i^3) + h_i + E_i^{\text{MF}}(t) - \Gamma\delta\dot{u}_i \quad (\text{S127})$$

In accordance with standard linear response, we assume that, in the absence of the external applied field, our displacement field has no dynamics (e.g.  $\langle \delta\dot{u}_i \rangle = \langle \delta\ddot{u}_i \rangle = 0$ ). After thermal and disorder averaging, this yields:

$$\left[ (k - \lambda) + \gamma p^2 + 3\gamma \overline{\langle \delta u_i(0)^2 \rangle} \right] p = 0 \quad (\text{S128})$$

which places a condition on  $p$ . Note that in the above expression, we have used the fact that  $\langle \delta\dot{u}_i \rangle = \langle \delta\ddot{u}_i \rangle = 0$  to replace  $\overline{\langle \delta u_i(t)^2 \rangle} = \overline{\langle \delta u_i(0)^2 \rangle}$ . Now, we add the above expression to our original equations of motion from which we can compute our auxiliary susceptibility:

$$\begin{aligned} M\delta\ddot{u}_i(t) &= -(\kappa - \lambda)\delta u_i(t) - \gamma \left[ 3p^2\delta u_i(t) + \delta u_i^3(t) + 3p(\delta u_i^2(t) - \overline{\langle \delta u_i(0)^2 \rangle}) \right] + h_i + E_i^{\text{MF}}(t) - \Gamma\delta\dot{u}_i(t) \\ &= -\left( \kappa - \lambda + 3\gamma \left[ \overline{\langle \delta u_i^2(0) \rangle} + p^2 \right] \right) \delta u_i(t) + h_i + E_i^{\text{MF}}(t) - \Gamma\delta\dot{u}_i(t) \end{aligned} \quad (\text{S129})$$

where in the second line, we approximated  $\delta u_i^2(t) = \overline{\langle \delta u_i^2(0) \rangle}$  and  $\delta u_i^3(t) = 3\overline{\langle \delta u_i^2(0) \rangle}\delta u_i(t)$ . From this, we can easily compute the auxiliary susceptibility:

$$\overline{\varphi_h}(\omega) = \frac{1}{M\Omega'^2 - M\omega^2 + i\omega\Gamma} \quad \text{where} \quad M\Omega'^2 = \left( \kappa - \lambda + 3\gamma \left[ \overline{\langle \delta u_i^2(0) \rangle} + p^2 \right] \right) \quad (\text{S130})$$

which immediately yields an expression for the retarded polarization correlation function (also called dielectric susceptibility):

$$\chi(\omega, \mathbf{q}) = \frac{1}{M\Omega_{\mathbf{q}}^2 - M\omega^2 + i\omega\Gamma} \quad (\text{S131})$$

with the phonon displacement mode appearing as a pole in the denominator:

$$M\Omega_{\mathbf{q}}^2 = M\Omega_0^2 + (v_0 - v_{\mathbf{q}}) = [M\Omega'^2 - (v_0 - \lambda)] + (v_0 - v_{\mathbf{q}}) \quad (\text{S132})$$

Now, to determine the parameter  $\lambda$ , we impose fluctuation-dissipation:

$$\overline{\langle u_i^2(0) \rangle} - \overline{\langle u_i(0) \rangle^2} = \frac{1}{N} \sum_{\mathbf{q}} \int \frac{d\omega}{2\pi} \coth\left(\frac{\beta\omega}{2}\right) \text{Im}[\chi(\omega, \mathbf{q})] = \frac{1}{N} \sum_{\mathbf{q}} \frac{1}{2M\Omega_{\mathbf{q}}} \coth\left(\frac{\beta\Omega_{\mathbf{q}}}{2}\right) \quad (\text{S133})$$

where we used that fact that  $\lim_{\Gamma \rightarrow 0} \text{Im}[\chi(\omega, \mathbf{q})] = \frac{\pi}{2M\omega} [\delta(\omega - \Omega_{\mathbf{q}}) + \delta(\omega + \Omega_{\mathbf{q}})]$ . Now, to close the self-consistency equations, we need expressions for  $\overline{\langle \delta u_i^2(0) \rangle}$ ,  $\overline{\langle u_i^2(0) \rangle}$ ,  $\overline{\langle u_i(0) \rangle^2}$ . To do so, first note that  $\overline{\langle \delta u_i^2(\omega) \rangle} = \overline{\langle u_i^2(\omega) \rangle} - p^2$ . Next, note that:  $\langle u_i(0) \rangle = p + \sum_j \chi_{ij}(0)h_j$  by definition. Therefore, this immediately yields that:

$$\overline{\langle u_i(0) \rangle^2} = p^2 + \frac{\Delta^2}{N} \sum_{\mathbf{q}} \chi(0, \mathbf{q})^2 = p^2 + \frac{\Delta^2}{N} \sum_{\mathbf{q}} \frac{1}{(M\Omega_{\mathbf{q}}^2)^2} \quad (\text{S134})$$

Therefore, we have closed the self-consistency equations. Eliminating  $\lambda$  and  $\Omega'$  from Eqs. S132 by using the definition of  $\Omega'$  in Eq. S130, we find the following self-consistency equations:

$$M\Omega_{\mathbf{q}}^2 = \left[ \kappa + 3\gamma(\overline{\langle u_i^2(0) \rangle} - p^2) - v_0 \right] + (v_0 - v_{\mathbf{q}}) \quad (\text{S135})$$

$$\overline{\langle u_i^2(0) \rangle} = p^2 + \frac{1}{N} \sum_{\mathbf{q}} \left[ \frac{1}{2M\Omega_{\mathbf{q}}} \coth\left(\frac{\beta\Omega_{\mathbf{q}}}{2}\right) + \frac{\Delta^2}{(M\Omega_{\mathbf{q}}^2)^2} \right] \quad (\text{S136})$$

where  $p$  can be determined from a thermodynamic analysis by finding minima of free energies. This is a very lengthy procedure (which was carried out in Ref. [9]) and so, for our purposes, we can pick  $p = 0$ . To compute the polarization correlations entering into the expression for  $1/T_1$ , we use Eq. S131 in the limit where  $\Gamma \rightarrow 0$ .

### Computation of Critical Temperature

Using the methods above, it is possible to compute a critical temperature for the para-to-ferroelectric transition that exists in the absence of disorder ( $\Delta = 0$ ). Recall that at the critical temperature, the mass of the transverse optical phonon mode goes to zero. Using Eq. S135, we can express the mode mass as:

$$M\Omega_0^2 = \left[ \kappa + 3\gamma(\overline{\langle u_i^2(0) \rangle} - p^2) - v_0 \right] \quad (\text{S137})$$

Moreover, in the absence of disorder and with  $p = 0$ , the fluctuation  $\overline{\langle u_i^2(0) \rangle}$  is found by Eq. S136 to be:

$$\overline{\langle u_i^2(0) \rangle} = \frac{1}{N} \sum_{\mathbf{q}} \left[ \frac{1}{2M\Omega_{\mathbf{q}}} \coth \left( \frac{\beta\Omega_{\mathbf{q}}}{2} \right) \right] \approx \frac{1}{N} \sum_{\mathbf{q}} \frac{k_B T}{M\Omega_{\mathbf{q}}^2} = \frac{1}{N} \sum_{\mathbf{q}} \frac{k_B T}{M\Omega_0^2 + (v_0 - v_{\mathbf{q}})} \quad (\text{S138})$$

We can solve for  $T_c$  by setting  $\Omega_0 = 0$  and plugging Eq. S138 into Eq. S137, yielding:

$$k_B T_c = \frac{v_0 - \kappa}{3\gamma} \times \left[ \frac{1}{N} \sum_{\mathbf{q}} \frac{1}{(v_0 - v_{\mathbf{q}})} \right]^{-1} \quad (\text{S139})$$

Note that this  $T_c$  does not indicate a transition in the relaxor case and is simply a reference temperature.

- 
- [1] K. Agarwal, R. Schmidt, B. Halperin, V. Oganessian, G. Zaránd, M. D. Lukin, and E. Demler, *Phys. Rev. B* **95**, 155107 (2017).
  - [2] V. Kozii, Z. Bi, and J. Ruhman, *Phys. Rev. X* **9**, 031046 (2019).
  - [3] B. I. Halperin, P. C. Hohenberg, and S.-k. Ma, *Phys. Rev. B* **10**, 139 (1974).
  - [4] B. I. Halperin, P. C. Hohenberg, and S.-k. Ma, *Phys. Rev. B* **13**, 4119 (1976).
  - [5] P. C. Hohenberg and B. I. Halperin, *Rev. Mod. Phys.* **49**, 435 (1977).
  - [6] S. Sachdev, *Handbook of Magnetism and Advanced Magnetic Materials* (2007).
  - [7] S. Sachdev, *Nuclear Physics B* **464**, 576 (1996), [arXiv:cond-mat/9509147 \[cond-mat\]](#).
  - [8] Q. Li, E. H. Hwang, and S. Das Sarma, *Phys. Rev. B* **82**, 235126 (2010).
  - [9] G. G. Guzmán-Verri, P. B. Littlewood, and C. M. Varma, *Phys. Rev. B* **88**, 134106 (2013).
  - [10] G. G. Guzmán-Verri and C. M. Varma, *Phys. Rev. B* **91**, 144105 (2015).
  - [11] G. G. G. Verri, *Theory of Relaxor Ferroelectrics* (University of California, Riverside, 2012).
  - [12] R. Brout and H. Thomas, *Physics Physique Fizika* **3**, 317 (1967).
  - [13] Y. Yafet, J. Kwo, and E. M. Gyorgy, *Phys. Rev. B* **33**, 6519 (1986).
  - [14] R. P. Erickson, *Phys. Rev. B* **46**, 14194 (1992).